

#### LIBRARIES MICHIGAN STATE UNIVERSITY EAST LANSING, MICH 48824-1048

1 = 32°5

3783

THESIS

## This is to certify that the thesis entitled

## SENSORLESS SPEED CONTROL OF INDUCTION MOTORS USING SLIDING MODE CONTROL STRATEGY

presented by

#### ATTAULLAH YOUSUF MEMON

has been accepted towards fulfillment of the requirements for the

Masters degree in Electrical Engineering

Major Professer's Signature

December 13,2004

Date

MSU is an Affirmative Action/Equal Opportunity Institution

PLACE IN RETURN BOX to remove this checkout from your record.

TO AVOID FINES return on or before date due.

MAY BE RECALLED with earlier due date if requested.

DATE DUE	DATE DUE	DATE DUE
SEP 1 8 2006		

6/01 c:/CIRC/DateDue.p65-p.15

# Sensorless Speed Control of Induction Motors Using Sliding Mode Control Strategy

By

Attaullah Yousuf Memon

## A THESIS

Submitted to
Michigan State University
in partial fulfillment of the requirements
for the degree of

MASTER OF SCIENCE

Department of Electrical and Computer Engineering

2004

## **ABSTRACT**

# Sensorless Speed Control of Induction Motors Using Sliding Mode Control Strategy

By

#### Attaullah Yousuf Memon

The field-oriented speed control of induction motors without mechanical sensors is considered. A sliding mode speed control algorithm is developed for the speed control that replaces the traditional PI controller. The traditional approach for the sensorless speed control of using flux and speed observers is augmented with a sixthorder nonlinear induction machine model that describes the motor in field-oriented coordinates. The model takes into consideration the errors in flux estimation. The flux regulation problem is addressed by following the traditional approach of using PI controllers. For the speed regulation problem, the machine model is simplified by assuming that the flux regulation takes place relatively fast and by employing a sliding mode controller that presents good performance against un-modeled dynamics, insensitivity to parameter variations, external disturbance rejection and fast dynamic response. A performance comparison of the developed sliding mode controller with the traditional PI controller is presented. The simulation presents the edge that the developed sliding mode controller has over its counterpart, a traditional PI controller. The analysis reveals the conditions under which the sliding mode controller provides effective speed control while preserving the closed-loop system stability under uncertain external load disturbances and reference speed variations.

Copyright © by

Attaullah Yousuf Memon

2004

To my father... and his fond memories

## **ACKNOWLEDGMENTS**

I am highly indebted to my advisor Dr. Hassan K. Khalil, whose keen insight and great vision in the subject provided me with invaluable advice for the work in this thesis. His encouragement and support, both morally and academically, made the time span of last several months truly memorable. I can not thank him enough for all he has done for me.

I would also like to thank Dr. Elias G. Strangas and Dr. Fang. Z. Peng for their valuable inputs to this work and for serving on the committee.

I would like to thank National University of Sciences and Technology (NUST), Pakistan, for the financial support throughout the tenure of my master's studies.

I am grateful to many friends for their help, throughout the ups and downs during the past many months, for providing me with hundreds of memorable moments to cherish.

And, I have no words to thank the very special person in my life, my mother, for her love and unconditional support, for everything she has done for me. I owe my gratitude to my best friends, my brother and my sister, for their love and encouragement, and to my wife, for all the things she has done for me.

## TABLE OF CONTENTS

LI	ST (	OF FIGURES	viii
1	Intr	roduction	1
	1.1	Why Sensorless Electric Drive?	2
	1.2	Speed Estimation in Induction Motor Drives	
	1.3	Scope of thesis work	4
2	Lite	erature Review	6
	2.1	The Induction Motor	6
	2.2	Principle of Operation	6
	2.3	Reference-Frame Transformation	8
	2.4	Frequency-Controlled Induction Motor Drives	11
		2.4.1 Static Frequency Changers	12
		2.4.2 Speed Control	13
	2.5	Vector Controlled Induction Motor Drives	17
		2.5.1 Principle of Field Oriented Control	18
3	Pre	vious Work	20
	3.1	Introduction	20
	3.2	Induction Motor Model	21
	3.3	Flux Observer	21
	3.4	Flux Regulation	23
	3.5	Speed Observer	23
	3.6	Speed Controller	26
4	Spe	ed Control Using Sliding Mode Control Strategy	32
	4.1	Introduction	32
		4.1.1 Sliding Mode Control	33
		4.1.2 Zero Dynamics and the Relative Degree of Nonlinear Systems .	35
		4.1.3 Regulation via Integral Control in Relative Degree-1 Systems .	38
	4.2	Sliding Mode Controller Design For the Induction Motor	39

		4.2.1	Zero Dynamics of the system	40
		4.2.2	Speed Regulation via Integral Control	45
5	Sim	ulatio	ns	59
	5.1	Perfor	mance Comparison - PI controller vs Sliding Mode Controller	59
		5.1.1	Designing PI Controllers for the Speed Control	60
		5.1.2	Sliding Mode Controller - Parameters	63
		5.1.3	Performance Comparison	64
6	Cor	iclusio	ns	77
B	BIBLIOGRAPHY			

## LIST OF FIGURES

2.1	Transformation equations as trigonometric relationships	9
3.1	Sensorless control of an induction motor using traditional PI controllers	30
4.1	A typical phase portrait under sliding mode control	34
4.2	Trajectory outside the boundary layer reach it in finite time and stay	
	inside thereafter	50
4.3	Sensorless control of an induction motor using sliding mode controller .	57
5.1	Simulation results with nominal parameters	65
5.2	Simulation results with 100 percent increase in $R_r$ and nominal $R_s$	67
5.3	Simulation results with 100 percent increase in $R_r$ and $R_s$	68
5.4	Simulation results for speed reversal under no load conditions with	
	nominal parameters	69
5.5	Simulation results for step load torque $\mathcal{T}_L$ with nominal parameters	70
5.6	Simulation results for sudden step load torque increase with nominal	
	parameters	71
5.7	Simulation results demonstrating loss of stability in case of PI con-	
	troller when under negative load torque with nominal parameters	72
5.8	Simulation results for step speed command with nominal parameters .	73
5.9	Simulation results for multi-step speed reduction with nominal param-	
	eters	74
5.10	Simulation results for monotonic speed reduction command with nom-	
	inal parameters	<b>7</b> 5

## CHAPTER 1

## Introduction

The induction motor is the motor of choice in several industrial applications due to its reliability, power-to-size ratio, ruggedness and relatively low cost. In the last few decades, the induction motor has evolved from being a constant speed motor to a variable speed, variable torque machine. DC motors had the advantage of precise speed control at the cost of many disadvantages, including but not limited to the maintenance requirements, complex structures and power limits. The induction motors are robust, smaller in size, almost maintenance free and possess a wide range of speeds when compared with the DC motors. Their mechanical dependability is due to the reason that there is no requirement of mechanical commutation (i.e. there are no brushes nor commutators to wear out as in the DC motors). Another advantage is that Induction Motors can be used in many volatile environments since no sparks are produced as is the case in the commutator of the DC motors.

However, the induction motor, by itself, presents a very challenging control problem. This is owing to the complex nature of issues that the induction motor presents;

- The dynamic model of the induction motor is nonlinear
- Certain state variables e.g. rotor fluxes are not measurable

• Due to the ohmic temperature rise, the rotor resistance varies considerably with a corresponding significant effect on the system dynamics

## 1.1 Why Sensorless Electric Drive?

Many variable-speed electrical drives used in general-purpose applications ranging from simple servo systems to complex traction systems require a capability of speed variation with a pre-defined performance standard. In such applications, it is necessary that the actual drive-speed measurements be available at every instant in order to control the drive effectively. For this reason, many different kinds of speed sensors have been used, including tacho generators, optical encoders, resolvers, etc. Elimination of such a requirement of having speed sensor on the motor shaft represents a cost advantage, and also enhances the reliability of the drive owing to the absence of a mechanical sensor and associated cable accessories.

The idea of developing efficient sensorless electric drives has gained considerable interest due to their low cost and dependability, since there is no further requirement of having a mechanical sensor to measure speed. Instead, the intrinsic motor electro-mechanical properties can be utilized to estimate the rotor position and/or speed. There are numerous methods that have been proposed by various researchers in this field over the last two decades. Of considerable significance are the collection of papers by Rajashekara et al [6], the tutorials by Lorenz [11] and Holtz [4], and the monographs by Leonhard [10] and Vas [14]. The identification of the rotor speed is generally based on measured terminal voltages and currents. Various dynamic models are used in order to estimate the magnitude and the spatial orientation of the magnetic flux vector and for this purpose open loop estimators or closed-loop observers are used, which usually differ with respect to accuracy,

robustness and sensitivity against model parameter variations.

## 1.2 Speed Estimation in Induction Motor Drives

There are two basic approaches for speed and position estimation in induction motors. The first approach uses the fundamental machine model to design model reference adaptive systems, nonlinear observers, extended Kalman filters, or adaptive observers. It has long been recognized that the challenging part in this approach is keeping a load stationary at (or near) zero flux frequency. The second approach uses secondary phenomena or the parasitic effects of the machine to develop methods that will be effective at low frequency.

In their recent work [8], Khalil and Strangas have identified some drawbacks associated with the analysis using the first approach that has been done so far and subsequently published by many researchers in this field. These are summarized here:

- Analysis is limited to local linear models; it is rare to find analysis that takes
   into consideration the nonlinearities of the system
- Model uncertainty is usually ignored in the analysis, even though the presence
  of such uncertainty (e.g. change of resistances with temperature) could change
  the conclusions in a fundamental way
- No analysis of the overall closed loop system. It is typical in methods based
  on rotor or flux position estimation that the analysis is limited to the position
  estimation problem itself with no analysis of the impact of the estimation error
  on the performance of the closed-loop system

The traditional field-oriented control [10, 9] is studied here, where a flux observer is used to estimate the rotor flux. The speed control problem is considered, where the motor speed is required to track a given speed command in the presence of an unknown load. The two key elements of the approach of [8] are:

- To keep track of the error in estimation of the rotor flux, field orientation is performed using the estimated flux angle and two additional state variables are added by projecting the flux estimation error into the field oriented coordinates
- A high-gain observer is used to estimate the speed from current measurements

With the use of these two key elements, a nonlinear model of the induction motor in the field-oriented coordinates was derived that formulates the flux and speed regulation problems. The flux regulation problem was addressed by using the traditional approach of using PI controllers. While addressing the speed regulation problem, the nonlinear induction motor model was simplified by assuming that the flux regulation takes place relatively fast and by using a high-gain PI controller to regulate the q-axis current to its command. This results in a third-order non-linear model in which the speed and two flux estimation errors are the state variables, the q-axis current is the control input and a speed estimate provided by the high-gain observer is the measured output. The analysis was limited to the design of PI controllers via linearization.

## 1.3 Scope of thesis work

This work is an extension of the analysis of the closed-loop system using the thirdorder non-linear model [8]. The goal here is to design a nonlinear feedback controller for the stator voltage  $v_s$  that uses only the measurements of the stator current  $i_s$ , such that the rotor speed  $\omega$  asymptotically tracks a bounded time-varying reference speed  $\omega_{ref}$ . Here, a nonlinear sliding-mode speed control algorithm is developed and implemented, and the analysis of the overall closed loop system is undertaken. The analysis provides a better insight into the speed control problem when the nonlinearities of the machine model are taken into account and presents certain bounds and conditions in which the developed speed control algorithm will work with a superior performance. Various machine operating situations are taken into account for the purpose of simulations using the developed speed control algorithm and the results obtained are compared with those obtained using the traditional PI control algorithm. The comparison simulations clearly indicate the edge that the developed speed control algorithm has over the traditional PI control.

## CHAPTER 2

## Literature Review

## 2.1 The Induction Motor

The induction motor was invented by Nikola Tesla (1856 - 1943) in 1888. It requires no electrical connections to the rotating member; the transfer of energy from the stationary member to the rotating member is by means of electro magnetic induction. A rotating magnetic field, produced by a stationary winding (called the stator), induces an alternating emf and current in the rotor. The resultant interaction of the induced rotor current with the rotating field of the stationary winding produces motor torque.

The Torque - Speed characteristic of an induction motor is directly related to the resistance and reactance of the rotor. Hence, different Torque - Speed characteristics may be obtained by designing rotor circuits with different ratios of rotor resistance to rotor reactance.

## 2.2 Principle of Operation

When a set of three-phase currents displaced in time from each other by angular intervals of 120 degrees is injected into a stator having a set of three-phase windings

displaced in space by 120 degrees electrical, a rotating magnetic field is produced [9]. This rotating magnetic field has a uniform strength and travels at an angular speed equal to its stator frequency. The rotating magnetic field in the stator induces electromagnetic forces in the rotor windings. As the rotor windings are short-circuited, currents start circulating in them, producing a reaction. As known from Lenz's law, the reaction is to counter the source of the rotor currents, i.e. the induced emfs in the rotor and, in turn, the rotating magnetic field itself. The induced emfs will be countered if the difference between the speed of the rotating magnetic field and the rotor becomes zero. The only way to achieve it is for the rotor to run in the same direction as that of the stator magnetic field and catch up with it eventually. When the differential speed between the rotor and magnetic field in the stator becomes zero, there's zero emf, and hence zero rotor currents resulting in zero torque production in the motor. Depending on the shaft load, the rotor will settle down to a speed  $\omega_r$  always less than the speed of the rotating magnetic field, called the Synchronous Speed of the machine  $\omega_s$ . The speed differential is known as the Slip Speed  $\omega_{sl}$ .

The Synchronous Speed of the machine  $\omega_s$  is given as

$$\omega_s = 2\pi f_s(rad/sec) \tag{2.1}$$

where  $f_s$  is the supply frequency.

The slip speed is given as

$$\omega_{sl} = \omega_s - \omega_r(rad/sec) \tag{2.2}$$

The differential speed between the stator magnetic field and rotor windings is the slip speed, and this is responsible for the frequency of the induced emfs in the rotor and hence the *rotor currents*.

The direction of rotation of an induction motor is dependant on the direction of rotation of the stator flux, which in turn is dependant on the phase sequence of the applied voltage.

## 2.3 Reference-Frame Transformation

The performance of an induction machine is generally described by a set of differential equations. Some of the machine inductances appearing in these equations are functions of the rotor speed and the coefficients of the differential equations that describe the behavior of the induction machine are generally time-varying. A change of variables is often used in order to reduce the complexity of these differential equations. A transformation refers the machine variables to a frame of reference that rotates at an arbitrary angular velocity and a particular transformation can readily be obtained from this transformation by simply assigning the speed of rotation of the reference frame of our choice.

A change of variables that formulates a transformation of the 3-phase variables to the arbitrary reference frame may be expressed as [12]

$$\mathbf{f}_{ados} = \mathbf{K}_s \mathbf{f}_{abcs} \tag{2.3}$$

where

$$(\mathbf{f}_{qdos})^T = [f_{qs}f_{ds}f_{os}] \tag{2.4}$$

$$(\mathbf{f}_{abcs})^T = [f_{as}f_{bs}f_{cs}] \tag{2.5}$$

$$\mathbf{K}_{s} = \frac{2}{3} \begin{pmatrix} \cos\theta & \cos(\theta - \frac{2\pi}{3}) & \cos(\theta + \frac{2\pi}{3}) \\ \sin\theta & \sin(\theta - \frac{2\pi}{3}) & \sin(\theta + \frac{2\pi}{3}) \\ \frac{1}{2} & \frac{1}{2} & \frac{1}{2} \end{pmatrix}$$

$$(2.6)$$

$$\omega = \frac{d\theta}{dt} \tag{2.7}$$

In the foregoing equations, f can represent any variable like voltage, flux-linkage or current. The frame of reference may rotate at any constant or varying angular velocity or it may remain stationary. It is convenient to visualize the transformation equations as the trigonometric relationships between variables as shown in Figure 2.1.

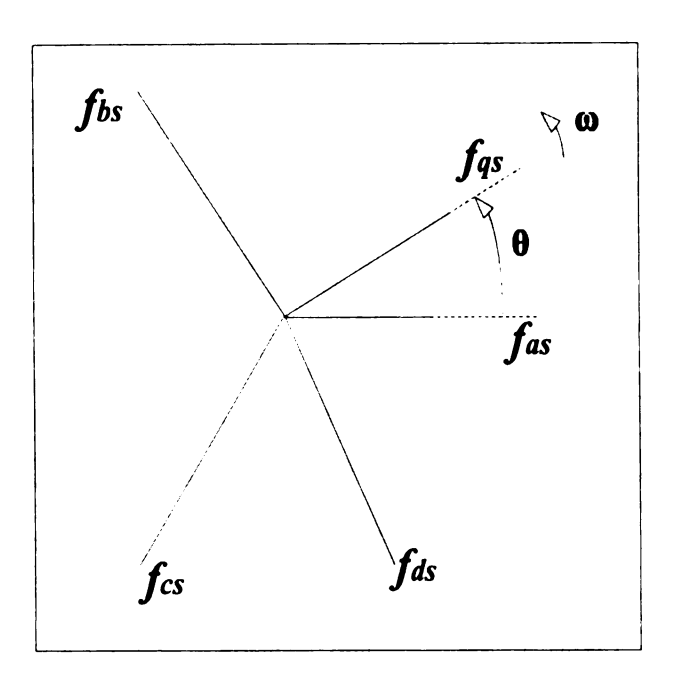


Figure 2.1. Transformation equations as trigonometric relationships

The equations of transformation may be thought of as if  $f_{qs}$  and  $f_{ds}$  variables are directed along the paths orthogonal to each other and rotating at an angular velocity  $\omega$ , whereupon  $f_{as}$ ,  $f_{bs}$  and  $f_{cs}$  may be considered as variables directed along stationary paths, each displaced by 120 degrees. If  $f_{as}$ ,  $f_{bs}$  and  $f_{cs}$  are resolved into  $f_{qs}$ , the first

row of equation (3.2) is obtained, and if  $f_{as}$ ,  $f_{bs}$  and  $f_{cs}$  are resolved into  $f_{ds}$ , the second row is obtained. The  $f_{0s}$  variables are not associated with the reference frame, instead, they are only related arithmetically to the abc variables, independent of  $\theta$ . Portraying the transformation as shown in Fig. 2.1 is particularly convenient when applying it to ac machines where the direction of  $f_{as}$ ,  $f_{bs}$  and  $f_{cs}$  may be thought of as the direction of the magnetic axes of the stator windings. Then, the direction of  $f_{qs}$  and  $f_{ds}$  can be considered as the direction of the magnetic axes of the new windings created by the change of variables. The reference frame transformation therefore simplifies the intricate equations involving 120 degree 3-phase variables into the 2-phase orthogonal variables.

#### Commonly used reference frames

The reference frames commonly used in the analysis of electric machines and power systems can be described as, the arbitrary, stationary, rotor and synchronous reference frames. The arbitrary reference frame can be defined as the one that can be assigned any given angular velocity corresponding to the fundamental frequency associated with a quantifiable variable like flux-linkage for example. The synchronous reference frame is the reference frame rotating at the electrical angular velocity corresponding to the fundamental frequency of the variables associated with the stationary circuits. In the case of ac machines, it is the electrical angular velocity of the air-gap rotating magnetic field established by stator currents of fundamental frequency.

#### Transformation between reference frames

Many times during the derivations and analyses it is convenient to relate variables in one reference frame to another reference frame directly, without involving *abc* variables in the transformation. This direct transformation takes the form of a *Vector Rotator* given as

$$\begin{pmatrix} cos(\theta_y - \theta_x) & -sin(\theta_y - \theta_x) \\ sin(\theta_y - \theta_x) & cos(\theta_y - \theta_x) \end{pmatrix}$$

where  $\theta_y$  and  $\theta_x$  represent the angular displacements associated with the reference frames involved with the inter-frame transformation.

## 2.4 Frequency-Controlled Induction Motor Drives

The speed of an induction motor is very near to its *synchronous speed*. The difference between the two being characterized by the *slip speed*. If the synchronous speed of the induction motor is changed, there is a corresponding change in the speed of the motor and this can be done by changing the supply frequency of the a.c. source. The relationship between the synchronous speed and the frequency is given by

$$\eta_s = \frac{120f_s}{P} \tag{2.8}$$

where  $\eta_s$  is the synchronous speed in rev/min,  $f_s$  is the supply frequency in Hz and P is the number of poles.

The a.c. supply available for the utility purposes is of a constant frequency and when an induction motor is operated with the utility supply, it runs at a constant speed. For the purpose of speed control, a frequency changer is required to change the speed of the induction motor. The electric motor drives which use frequency changers to achieve the speed control are referred to as *Frequency-Controlled Electric Drives*.

#### 2.4.1 Static Frequency Changers

The static frequency changers can be broadly classified as *Direct* and *Indirect static* frequency changers. The direct frequency changers are some times called as Cycloconverters. These convert the a.c. supply source frequency to a variable frequency. The output frequency typically ranges from 0 to  $0.5f_s$ , and for the better waveform control of the output voltage, the frequency is limited to  $0.33f_s$ . The smaller range of frequency variation is suitable for low-speed and large-power applications.

For a majority of applications, a wide frequency range is desirable due to the requirements over the desired speed range. In such applications, the Indirect frequency conversion methods are employed. An indirect frequency changer consists of two power conversion stages; first stage is Rectification (ac to dc) and the second stage is *Inversion* (dc to ac). The indirect frequency changers are broadly classified depending on the source that supplies the input power to them and that can either be a voltage source or a current source. In both cases, the power input is kept to a specified constant. The output frequency becomes independent of the input supply frequency by means of the dc link. Various configurations of the indirect frequency changers have evolved keeping in view the diversity of applications. these only differ in the way the two power conversion stages are incorporated. The more common configurations are the so called PWM inverter fed induction motor drive, Variable-Voltage-Variable-frequency (VVVF) induction motor drive and Variable-Current-Variable-frequency (VCVF) induction motor drive. A detailed description of the current and voltage source static frequency changers and the current and voltage source inverters can be found in [9].

#### 2.4.2 Speed Control

For the inverter-driven induction motor, the speed control is effectively achieved by means of variable frequency. However, apart from the frequency, the applied voltage also needs be varied so that the air gap flux can be maintained at a constant value without letting it to saturate. It is well known that in order to maintain the air gap flux constant, the ratio between the phase voltage and the supply frequency is to be maintained to a constant value [9, 10]. Therefore, whenever stator frequency is changed to obtain speed control, the stator input voltage has to be changed accordingly to maintain the air gap flux at a constant value.

The requirement of keeping the ratio between the stator voltage and the stator frequency constant, actually compounds the speed control problem in an induction machine. This, in fact, is the difference between the speed control problem of an induction motor and a dc motor, which requires only the voltage control for the purpose, and the simplicity of the control problem made it preferable machine in many applications until early 1980s.

Various speed control strategies have been formulated for the induction machine, depending upon how the voltage-to-frequency ratio is implemented. The more important and commonly employed speed control strategies are precisely revisited here. Further details about these control strategies can be found in [9, 12]. The commonly employed speed control strategies for the induction machines are:

- 1. Constant Volts/Hz Control
- 2. Constant Slip-speed Control
- 3. Vector Control or Field-oriented Control

The speed control strategy developed here is based on the *Vector control* or the *Field Oriented Control*. Further discussion on the vector control is presented in the next section.

#### Constant Volts/Hz Control

The constant volts/Hz control is primarily designed to accommodate variable speed commands by using the inverter to apply a voltage of correct magnitude and frequency so as to approximately achieve the commanded speed without the use of speed feedback. Therefore, it is safe to say that the simplest and the least expensive induction motor drive strategy is constant volts/Hz control.

The speed control strategy relies on two foundations. One of them is that the torque-speed characteristic of an induction machine suggests that the electrical rotor speed of an induction machine is very near to the synchronous speed and hence has a direct relationship to the electrical frequency. Thus, by controlling the frequency, the speed can be controlled. The second foundation is based upon the phase-voltage equation that may be expressed as [12]

$$v_{as} = r_s i_{as} + \frac{d\lambda_{as}}{dt} \tag{2.9}$$

For steady-state conditions at intermediate to high speeds wherein the flux-linkage term dominates the resistive term in the voltage equation, the magnitude of the applied voltage is related to the magnitude of the stator flux-linkage by

$$V_s = \omega_e \Lambda_s \tag{2.10}$$

which suggests that in order to maintain constant flux linkage without any saturation, the stator voltage magnitude should be proportional to the frequency. The advantages of this control strategy are that it is simple and relatively inexpensive because of being an open loop control solution and that the speed can be controlled to a degree without using speed feedback. This, in turn, indicates a drawback of this control strategy; because it is open loop, some speed error will occur, particularly at low speeds.

#### Constant Slip-speed Control

In Constant Slip-speed Control, the drive system is designed so as to accept a torque command input and hence the system demands an additional feedback loop requiring the use of a speed sensor. The method is highly robust with respect to changes in machine parameters and results in high efficiency of both the machine itself and the inverter at the cost of somewhat sluggish response in closed-loop speed control situations.

The constant slip-speed control is inherently a current source based control strategy which offers the advantage that as the current is readily controlled and limited, the drive becomes extremely robust. However, this comes at an expense that the control strategy requires phase current feedback.

One of the simplest strategies for current control operation is to utilize a fixed slip-frequency, defined as

$$\omega_s = \omega_e - \omega_r \tag{2.11}$$

Which suggests that many different optimizations of the machine performance can readily be obtained by appropriately selecting the slip frequency  $\omega_s$ , including achieving the optimal torque for a given value of stator current (maximum torque per ampere) as well as the maximum efficiency [12].

#### Field-oriented Control

Field-oriented control provides the advantages of smooth motion at slow speeds as well as the efficient operation at high speeds. In many motor drive systems, it is desirable to make the drive act as a torque transducer wherein the electromagnetic torque can nearly instantaneously be made equal to a torque command. In such a system, speed control is dramatically simplified because the electrical dynamics of the drive become irrelevant to the speed control problem. There are a number of permutations of this kind of control strategy, broadly known as *Field Oriented Control*, and these include- stator flux-oriented, rotor flux-oriented, and air-gap flux-oriented control. Within these types, there are direct and indirect methods of implementations.

In the ideal field-oriented control, the current space vector is fixed in magnitude and direction (in quadrature) with respect to the rotor, irrespective of its rotation. This isolates the controllers from the time variant winding currents and voltages, and therefore eliminates the limitation of controller frequency response and phase shift on motor torque and speed. Using Field Oriented Control, the quality of current control is largely unaffected by speed of rotation of the motor.

The motor currents and voltages are manipulated in the d-q reference frame of the rotor. This means that measured motor currents must be mathematically transformed from the three-phase static reference frame of the stator windings to the two axis rotating d-q reference frame. Similarly, the voltages to be applied to the motor are mathematically transformed from the d-q frame of the rotor to the three phase reference frame of the stator before they can be used for PWM output. It is these reference frame transformations, which generally require the fast math capability of a DSP or a high performance processor, which are the heart of

### 2.5 Vector Controlled Induction Motor Drives

Various speed control strategies employed for the induction motors generally provide a good steady-state response. However, many of the control strategies present poor dynamic response and the cause of such poor dynamic response is found to be that the air-gap flux linkages deviate from their set values, both in magnitude and in phase. These variations in the flux linkages have to be controlled by the magnitude and frequency of the stator and rotor phase currents and their instantaneous phases. The oscillations in the air-gap flux linkages result in oscillations in electromagnetic torque and generally reflect as speed oscillations. Further, these result in large excursions of stator currents and present a requirement of larger peak ratings on inverters and converters that eliminate the cost advantage that ac drives have over their counterpart dc drives.

Induction Motor drives basically require a coordinated control of stator currents - in magnitudes, in frequencies and in phases - making it a complex and intricate control problem. However, it is possible to have an independent control of the flux and torque for the induction motor drives as in the dc drives. The stator current can be resolved along the rotor flux linkages and the component along the rotor flux linkages is the field producing current. But, this calculation requires the instantaneous position of the rotor flux linkages and if this is made available, the control problem simplifies to the similar one for the separately-excited dc drives. Since, the control is achieved in field coordinates, therefore, it is generally referred to as *Field Oriented Control* and because it relates to the control of the rotor flux linkages, it is also known as *Vector Control* [9].

### 2.5.1 Principle of Field Oriented Control

For the purpose of explaining principle of Field Oriented Control, it is assumed that the position of the rotor flux linkage  $\lambda_r$  is known and it is at an angle  $\rho$  from a stationary frame of reference. The three stator currents can be transformed into q and d axes currents in the synchronous reference frames by using the transformation

$$\begin{pmatrix} i_{qse} \\ i_{dse} \end{pmatrix} = \frac{2}{3} \begin{pmatrix} \sin\rho & \sin(\rho - \frac{2\pi}{3}) & \sin(\rho + \frac{2\pi}{3}) \\ \cos\rho & \cos(\rho - \frac{2\pi}{3}) & \cos(\rho + \frac{2\pi}{3}) \end{pmatrix} \begin{pmatrix} i_{as} \\ i_{bs} \\ i_{cs} \end{pmatrix}$$
(2.12)

from which the stator current  $i_s$  can be derived as

$$i_s = \sqrt{(i_{qse})^2 + (i_{dse})^2}$$
 (2.13)

and the stator current angle is given as

$$\theta_s = tan^{-1}(\frac{i_{qse}}{i_{dse}}) \tag{2.14}$$

where  $i_{qse}$  and  $i_{dse}$  are the q and d axes currents in the synchronous reference frames that are obtained by projecting the stator current on the q and d axes respectively.

The current  $i_s$  is responsible for producing the rotor flux  $\lambda_r$  and electromagnetic torque  $T_e$ . Resolving the stator current  $i_s$  along  $\lambda_r$  provides the field producing component  $i_f$  and the perpendicular component is the torque producing component  $i_T$ . By writing rotor flux linkages and torque in terms of these components as [9]

$$\lambda_r \propto i_f$$
 (2.15)

$$T_c \propto \lambda_r i_T \propto i_f i_T \tag{2.16}$$

it can be seen that the orientation of  $\lambda_r$  in synchronous reference frames presents the flux and torque producing components of the stator current  $i_s$  as dc quantities and, therefore, they are ideal for use as control variables.

The crucial thing to the implementation of the field oriented control is the acquiring of the instantaneous rotor flux angle  $\rho$ , which can be written as

$$\rho = \int (\omega_r + \omega_{sl})dt = \int \omega_s dt \tag{2.17}$$

and the field oriented control schemes are classified based on how  $\rho$  is acquired. If  $\rho$  is calculated by using terminal voltages and currents, then it is known as Direct Vector Control. On the other hand, if  $\rho$  is obtained by using rotor position measurements and/or using estimators or observers with only using machine parameters, then such a scheme is known as Indirect Vector Control.

A detailed discussion on the modeling, analysis and control schemes pertaining to the vector control of induction motors is provided in [9], where a number of direct and indirect vector control algorithms are presented for various applications.

## CHAPTER 3

## **Previous Work**

### 3.1 Introduction

The previous work [8] is reviewed in this chapter. It utilizes the fundamental induction machine model to design nonlinear observers for flux and speed estimation. A sixth-order nonlinear model of the induction machine is derived that describes the motor in field-oriented coordinates. The model takes into consideration the error in flux estimation. The flux regulation problem is addressed by following the traditional approach of using PI controllers. For the speed regulation problem, the machine model is simplified by assuming that the flux regulation takes place relatively fast and by using a PI controller to regulate the q-axis current to its command. A third-order nonlinear model is derived. Using this third-order nonlinear model, the speed regulation problem using a traditional PI controller is considered. The analysis presents conditions pertaining to the design of control for sensorless operation of induction motors. It reveals an important role played by the steady-state product of the flux frequency and the q-axis current in determining the control properties of the system.

## 3.2 Induction Motor Model

The Induction Motor is represented in stator frame of reference by the equations [9]

$$\frac{d}{dt}\lambda_r = \left(-\frac{R_r}{L_r}I + p\omega J\right)\lambda_r + \frac{R_r}{L_r}L_m i_s \sigma \tag{3.1}$$

$$L_s \frac{d}{dt} i_s = -\frac{L_m}{L_r} \left( -\frac{R_r}{L_r} I + p\omega J \right) \lambda_r - \left( R_s + \frac{R_r L_m^2}{L_r^2} \right) i_s + v_s$$
 (3.2)

$$m\frac{d\omega}{dt} = -\frac{3pL_m}{2L_r}\lambda_r^T J i_s - b_1 \omega - \frac{1}{m}T_L \tag{3.3}$$

where  $\lambda_r \in R^2$  is the rotor flux,  $i_s \in R^2$  is the stator current,  $v_s \in R^2$  is the stator voltage, and  $\omega$  is the rotor speed. The parameters  $L_r, L_s$  and  $L_m$  denote the rotor, stator, and mutual inductances,  $\sigma = 1 - L_m^2/L_sL_r$  is the leakage parameter,  $R_r$  and  $R_s$  are rotor and stator resistances, m is the rotor's moment of inertia,  $b_1$  is a friction coefficient, and p is the number of pole pairs. The resistance  $R_s$  which represents stator resistance,  $R_r$  which represents rotor resistance, the moment of inertia m, and the friction coefficient  $b_1$  are treated as uncertain parameters with  $\hat{R}_s, \hat{R}_r, \hat{m}$  and  $\hat{b}_1$  as their nominal values, respectively. The load torque  $T_L$  will be treated as a bounded time-varying disturbance.

The  $2 \times 2$  matrices I and J are defined by

$$I = \begin{pmatrix} 1 & 0 \\ 0 & 1 \end{pmatrix} \quad , \quad J = \begin{pmatrix} 0 & -1 \\ 1 & 0 \end{pmatrix}$$

## 3.3 Flux Observer

For the purpose of designing the controller, the field-orientation along the rotor flux  $\lambda_r$  is considered. Since  $\lambda_r$  is not measured, an open loop observer [15]

$$\frac{d}{dt}\hat{\lambda}_r = \left(-\frac{\hat{R}_r}{L_r}I + p\omega_{ref}J\right)\hat{\lambda}_r + \frac{\hat{R}_r}{L_r}L_m i_s \tag{3.4}$$

is used to estimate  $\lambda_r$ . The flux observer duplicates the flux equation (3.1), with the unavailable speed  $\omega$  replaced by its reference  $\omega_{ref}$ . Orienting the vectors  $\hat{\lambda}_r$ ,  $i_s$ ,  $v_s$  and  $e = \hat{\lambda}_r - \lambda_r$  along the vector  $\hat{\lambda}_r$ , and denoting the direct-axis components by  $\lambda_d$ ,  $i_d$ ,  $v_d$  and  $e_d$ , respectively, and the quadrature-axis components by  $\lambda_q(=0)$ ,  $i_q$ ,  $v_q$  and  $e_q$ , respectively, the motor can be represented by the following sixth-order nonlinear model [8].

$$\frac{d\lambda_d}{dt} = -\hat{\alpha_r}\lambda_d + \hat{\alpha_r}L_m i_d \tag{3.5}$$

$$\frac{di_d}{dt} = \alpha_r \beta \lambda_d - (\alpha_s \eta + \alpha_r \beta L_m) i_d + p \omega_{ref} i_q + \hat{\alpha_r} L_m i_q^2 / \lambda_d$$

$$+\gamma v_d - \alpha_r \beta e_d - \beta p \omega e_q \tag{3.6}$$

$$\frac{di_q}{dt} = -\beta p\omega \lambda_d - p\omega_{ref}i_d - (\alpha_s \eta + \alpha_r \beta L_m)i_q - \hat{\alpha_r} L_m i_d i_q / \lambda_d$$

$$+\gamma v_q + \beta p \omega e_d - \alpha_r \beta e_q \tag{3.7}$$

$$\frac{d\omega}{dt} = \mu[i_q(\lambda_d - e_d) + i_d e_q] - b\omega - T_L/m$$
 (3.8)

$$\frac{de_d}{dt} = -\alpha_r e_d + (p\omega_{ref} - p\omega + \hat{\alpha_r} L_m i_q / \lambda_d) e_q$$

$$+\left(\hat{\alpha_r} - \alpha_r\right)\left(L_m i_d - \lambda_d\right) \tag{3.9}$$

$$\frac{de_q}{dt} = -(p\omega_{ref} - p\omega + \dot{\alpha_r}L_m i_q/\lambda_d)e_d - \alpha_r e_q 
+ (\dot{\alpha_r} - \alpha_r)L_m i_q + p(\omega_{ref} - \omega)\lambda_d$$
(3.10)

where

$$\alpha_r = \frac{R_r}{L_r} , \ \hat{\alpha_r} = \frac{\hat{R_r}}{L_r}, \ \alpha_s = \frac{R_s}{L_s} , \ b = \frac{b_1}{m}$$
$$\beta = \frac{1-\sigma}{\sigma L_m}, \ \gamma = \frac{1}{\sigma L_s}, \ \eta = \frac{1}{\sigma}, \ \mu = \frac{3pL_m}{2mL_s}$$

For the later use, define

$$\hat{\alpha_s} = \frac{\hat{R_s}}{L_s}, \ \hat{\mu} = \frac{3pL_m}{2\hat{m}L_r}, \ \hat{b} = \frac{b_1}{\hat{m}}$$

In the foregoing equations,  $\lambda_d$ ,  $i_d$ , and  $i_q$  are available for feedback, as they can be calculated from  $i_s$  and  $\hat{\lambda}$ , while  $\omega$ ,  $e_d$  and  $e_q$  are not available.

### 3.4 Flux Regulation

In field orientation, the flux  $\lambda_d$  is regulated to a reference flux  $\lambda_{ref} > 0$ , which is taken as a constant. By viewing  $(-\alpha_r\beta e_d - \beta p\omega e_q)$  as a disturbance input to equation (3.6), the equations (3.5) and (3.6) can be used to design a state feedback controller for  $v_d$  to regulate  $\lambda_d$  to  $\lambda_{ref}$ . There are several methods available to design such a controller. The traditional approach of using two PI controllers [10] is considered here.

First,  $i_d$  is viewed as a control input to equation (3.5) and the PI controller is designed as

$$I_d^* = \frac{(K_{fp}s + K_{fi})}{s} [\lambda_{ref} - \lambda_d]$$

And then, the second PI controller is designed as

$$V_d = \frac{(K_{dp}s + K_{di})}{s} [I_d^* - I_d]$$

With tight feedback loops, the regulation of  $\lambda_d$  to  $\lambda_{ref}$  can be ensured for a wide range of variation of the term

$$p\omega_{ref}i_q + \hat{\alpha_r}L_m i_q^2/\lambda_d + \gamma v_d - \alpha_r\beta e_d - \beta p\omega e_q$$

which acts as an input on the right-hand side of equation (3.6). The design should ensure that  $\lambda_d$  starts at a positive value and approaches  $\lambda_{ref}$  monotonically so that  $\lambda_d$  is always positive. The initial conditions of  $\lambda_d$  are determined by the initial conditions of the flux observer (3.4).

### 3.5 Speed Observer

Sensorless operation of an Induction Motor essentially requires us to use an observer to measure the rotor speed, as no other means are available to measure the rotor speed online. The high-gain observer [7] is a technique that works for a wide class

of nonlinear systems and guarantees that the output feedback controller recovers the performance of a state feedback controller when the observer gain is sufficiently high. A high-gain observer is utilized here to estimate the rotor speed. Towards that end, rewriting equations (3.7) and (3.8) as

$$\frac{di_q}{dt} = -\beta p\omega \lambda_d - f_1(\lambda_d, i_d, i_q, w_{ref}) + \gamma v_q + \delta_1$$
(3.11)

$$\frac{di_q}{dt} = -\beta p\omega \lambda_d - f_1(\lambda_d, i_d, i_q, w_{ref}) + \gamma v_q + \delta_1$$

$$\frac{d\omega}{dt} = \hat{\mu} i_q \lambda_d - \hat{b}\omega + \delta_2$$
(3.11)

where

$$f_1(\lambda_d, i_d, i_q, \omega_{ref}) = p\omega_{ref}i_d + (\hat{\alpha_s}\eta + \hat{\alpha_r}\beta L_m)i_q + \hat{\alpha_r}L_m i_d i_q/\lambda_d$$

is available online, and  $\delta_1$ ,  $\delta_2$  are uncertain terms given by

$$\delta_1 = [(\hat{\alpha_s} - \alpha_s)\eta + (\hat{\alpha_r} - \alpha_r)\beta L_m]i_q + \beta p\omega e_d - \alpha_r\beta e_q$$
  
$$\delta_2 = (\mu - \hat{\mu})i_q\lambda_d + \mu(-i_qe_d + i_de_q) - (b - \hat{b})\omega - T_L/m$$

The change of variables

$$\Omega = \omega - \frac{\delta_1}{\beta p \lambda_d} 
= \left(\frac{\lambda_d - e_d}{\lambda_d}\right) - \frac{1}{\beta p \lambda_d} \left\{ \left[ (\hat{\alpha_s} - \alpha_s)\eta + (\hat{\alpha_r} - \alpha_r)\beta L_m \right] i_q - \alpha_r \beta e_q \right\}$$
(3.13)

brings equations (3.11) and (3.12) into the form

$$\frac{di_q}{dt} = -\beta p \omega \lambda_d - f_1(\lambda_d, i_d, i_q, \omega_{ref}) + \gamma v_q$$
(3.14)

$$\frac{d\omega}{dt} = \hat{\mu}i_q\lambda_d - \hat{b}\omega + \delta_3 \tag{3.15}$$

where

$$\delta_3 = \delta_2 - \frac{\hat{b}\delta_1}{\beta p \lambda_d} - \frac{d}{dt} (\frac{\delta_1}{\beta p \lambda_d}) \triangleq f_2(\lambda_d, i_d, i_q, \omega_{ref}, e_d, e_q, T_L)$$

and  $f_2$  is a continuous function of its arguments. The change of variables (3.13) is invertible provided  $\lambda_d - e_d \neq 0$ . The high-gain observer, then, is represented by the equations

$$\frac{d\hat{i}_q}{dt} = -\beta p \lambda_d \hat{\Omega} - f_1(\lambda_d, i_d, i_q, \omega_{ref}) + \gamma v_q + (\frac{\alpha_1}{\varepsilon})(i_q - \hat{i}_q)$$
 (3.16)

$$\frac{d\hat{i}_q}{dt} = -\beta p \lambda_d \hat{\Omega} - f_1(\lambda_d, i_d, i_q, \omega_{ref}) + \gamma v_q + (\frac{\alpha_1}{\varepsilon})(i_q - \hat{i}_q) \qquad (3.16)$$

$$\frac{d\hat{\Omega}}{dt} = \hat{\mu} i_q \lambda_d - \hat{b}\hat{\Omega} - (\frac{\alpha_2}{\varepsilon^2 p \beta \lambda_d})(i_q - \hat{i}_q) \qquad (3.17)$$

where  $\varepsilon$  is a small positive parameter and  $\alpha_1$  and  $\alpha_2$  are positive constants that assign the roots of  $s^2 + \alpha_1 s + \alpha_2 = 0$  at desired locations in the left-half s - plane. The scaled estimation errors

$$\eta_1 = \frac{i_q - \hat{i}_q}{\varepsilon} , \ \eta_2 = \Omega - \hat{\Omega}$$

satisfy the equations

$$\varepsilon \dot{\eta}_1 = \alpha_1 \eta_1 - \beta p \lambda_d \eta_2 \tag{3.18}$$

$$\varepsilon \dot{\eta}_2 = -(\frac{\alpha_2}{\beta p \lambda_d}) \eta_1 - \varepsilon \hat{b} \eta_2 - \varepsilon \delta_3 \tag{3.19}$$

For small  $\varepsilon$ , the closed loop system will behave as a singularly perturbed system, with  $\eta_1$  and  $\eta_2$  as the fast variables. The essence of the singular perturbation theory [7], is that when we face a perturbation problem that is characterized by discontinuous dependance of the system properties on the perturbation parameter  $\varepsilon$ , then the discontinuity of solutions caused by singular perturbations can be avoided if analyzed in separate time scales. According to singular perturbation theory [13], the stability of the fast dynamics is determined by the matrix

$$\left(\begin{array}{cc}
-\alpha_1 & -\beta p \lambda_d \\
\frac{\alpha_2}{\beta p \lambda_d} & 0
\end{array}\right)$$

in which  $\lambda_d > 0$  is treated as a constant. The characteristic equation of this matrix is  $s^2 + \alpha_1 s + \alpha_2 = 0$ ; hence, it is Hurwitz by design. From the high-gain observer

theory [1], it is known that if the control input  $v_s$  is bounded uniformly in  $\varepsilon$ , then the estimation error  $\Omega - \hat{\Omega}$  will be  $O(\varepsilon)$  after a short transient period  $[0, T(\varepsilon)]$ , where  $\lim_{\varepsilon \to 0} T(\varepsilon) = 0$ .

## 3.6 Speed Controller

The design of speed controller can be simplified by reducing the order of the system. First, it is assumed that the flux regulator acts fast enough to regulate  $\lambda_d$  to its constant reference  $\lambda_{ref}$ . This assumption allows us to take  $\lambda_d = \lambda_{ref}$  and, therefore,  $i_d = \frac{\lambda_{ref}}{Lm}$  leads to dropping equations (3.5) and (3.6). Also, it can be seen from equation (3.7) that for any current command  $i_q^*$ , we can design  $v_q$  as the PI controller

$$V_{q} = \frac{(K_{qp}s + K_{qi})}{s} [I_{q}^* - I_{q}]$$

with sufficiently large gains to regulate  $i_q$  to  $i_q^*$ . This allows us to view  $i_q$  as the control input. Thus, the speed controller can be designed using the third-order model

$$\frac{d\epsilon_d}{dt} = -\alpha_r \epsilon_d + (p\omega_{ref} - p\omega + \hat{\alpha_r} L_m i_q / \lambda_{ref}) \epsilon_q \qquad (3.20)$$

$$\frac{de_q}{dt} = -(p\omega_{ref} - p\omega + \hat{\alpha_r}L_m i_q/\lambda_{ref})\epsilon_d - \alpha_r \epsilon_q$$

$$+ (\hat{\alpha_r} - \alpha_r) L_m i_q + p(\omega_{ref} - \omega) \lambda_{ref}$$
 (3.21)

$$\frac{d\omega}{dt} = \mu \left\{ i_q (\lambda_{ref} - e_d) + \frac{\lambda_{ref}}{L_m} e_q \right\} - b\omega - T_L/m$$
 (3.22)

$$\Omega = \left(\frac{\lambda_{ref} - e_d}{\lambda_{ref}}\right) \omega + \frac{\alpha_r e_q}{p \lambda_{ref}} - a i_q$$
 (3.23)

where  $\Omega$  is viewed as the measured output and,

$$a = \frac{(\hat{\alpha_s} - \alpha_s)\eta + (\hat{\alpha_r} - \alpha_r)\beta L_m}{\beta p \lambda_{ref}}$$

The goal is to have  $\Omega$  track  $\omega_{ref}$ .

It is natural to use integral control to ensure zero steady-state error when  $\omega_{ref}$  and  $T_L$  are constant [7]. Under the condition,  $\Omega = \omega_{ref}$ , the equilibrium equations are

$$0 = -\alpha_r e_d + (p\omega_{ref} - p\bar{\omega} + \hat{\alpha_r} L_m \bar{i_q} / \lambda_{ref}) e_q$$
 (3.24)

$$0 = -(pw_{ref} - p\bar{w} + \hat{\alpha_r}L_m\bar{i_q}/\lambda_{ref})\bar{e_d} - \alpha_r\bar{e_q}$$

$$+(\hat{\alpha_r} - \alpha_r)L_m \bar{i_q} + p(\omega_{ref} - \bar{\omega})\lambda_{ref}$$
 (3.25)

$$0 = \mu[\bar{i_q}(\lambda_{ref} - \bar{e_d}) + \frac{\lambda_{ref}}{L_m}\bar{e_q}] - b\bar{\omega} - T_L/m$$
(3.26)

$$\Omega = \left(\frac{\lambda_{ref} - \bar{e_d}}{\lambda_{ref}}\right)\bar{\omega} + \frac{\alpha_r \bar{e_q}}{p\lambda_{ref}} - a\bar{i_q}$$
(3.27)

Solving equations (3.24) and (3.25) for  $\bar{e_d}$  and  $\bar{e_q}$  in terms of  $\bar{i_q}$  and  $\bar{\omega} \doteq \bar{\omega} - \omega_{ref}$  and substituting in equation (3.27), it can be shown that

$$(-p\tilde{\omega} + \frac{\hat{\alpha_r}L_m\bar{l_q}}{\lambda_{ref}})(-p\tilde{\omega} + \frac{(\hat{\alpha_r} - \alpha_r)L_m\bar{l_q}}{\lambda_{ref}})\omega_c = -\frac{(\hat{\alpha_s} - \alpha_s)\eta\Delta\bar{l_q}}{\beta\lambda_{ref}}$$

where

$$\omega_c = p\omega_{ref} + \frac{\hat{\alpha_r}L_m\bar{i_q}}{\lambda_{ref}}$$
 and  $\Delta = \alpha_r^2 + (-p\tilde{\omega} + \frac{\hat{\alpha_r}L_m\bar{i_q}}{\lambda_{ref}})^2$ 

To gain insight into the problem, the case is considered when  $\hat{\alpha_s} = \alpha_s$ , for which the preceding equation reduces to

$$(-p\tilde{\omega} + \frac{\hat{\alpha_r}L_m\bar{i_q}}{\lambda_{ref}})(-p\tilde{\omega} + \frac{(\hat{\alpha_r} - \alpha_r)L_m\bar{i_q}}{\lambda_{ref}})\omega_c = 0$$

Assuming that  $\omega_c \neq 0$ , the equation has two solutions:

$$\tilde{\omega} = \frac{(\hat{\alpha_r} - \alpha_r)L_m\bar{i_q}}{p\lambda_{ref}}$$
 or  $\tilde{\omega} = \frac{\hat{\alpha_r}L_m\bar{i_q}}{p\lambda_{ref}}$ 

It is clear that the first solution is the one which yields zero steady-state error in the nominal case when  $\hat{\alpha_r} = \alpha_r$ . The equilibrium point corresponding to this solution is

$$\bar{e}_d = 0$$

$$\bar{\epsilon}_{q} = 0$$

$$\bar{i}_{q} = \frac{b\omega_{ref} + T_{L}/m}{\mu\lambda_{ref} - \frac{b(\alpha_{r} - \alpha_{r})L_{m}}{p\lambda_{ref}}}$$

$$\bar{\omega} = \omega_{ref} + \frac{(\alpha_{r} - \alpha_{r})L_{m}\bar{i}_{q}}{p\lambda_{ref}}$$
(3.28)

In order to see whether a PI controller can stabilize this equilibrium point, the equations (3.20)-(3.23) are linearized at this equilibrium point, to obtain the linear model

$$\dot{x} = Ax + B(i_q - \bar{i}_q)$$

$$\Omega - \omega_{ref} = Cx + D(i_q - \bar{i}_q)$$

where

$$A = \begin{pmatrix} -\alpha_r & \frac{\alpha_r L_m \bar{i}_q}{\lambda_{ref}} & 0 \\ -\frac{\alpha_r L_m \bar{i}_q}{\lambda_{ref}} & -\alpha_r & -p\lambda_{ref} \\ \mu i_q & \frac{\mu \lambda_{ref}}{L_m} & -b \end{pmatrix}$$

$$B = \begin{pmatrix} 0 \\ (\hat{\alpha}_r - \alpha_r) L_m \\ \mu \lambda_{ref} \end{pmatrix}$$

$$C = \begin{pmatrix} -\frac{\bar{\omega}}{\lambda_{ref}} & \frac{\alpha_r}{p\lambda_{ref}} & 1 \end{pmatrix}$$

and

$$D = \left( -\frac{(\hat{\alpha}_r - \alpha_r)L_m}{p\lambda_{ref}} \right)$$

with the transfer function

$$G(s) = C(sI - A)^{-1}B + D = \frac{n(s)}{d(s)}$$

in which

$$n(s) = \mu \lambda_{ref} [s^2 + \alpha_r s + \frac{\omega_c \alpha_r L_m \bar{i_q}}{\lambda_{ref}}] [1 - \frac{(\hat{\alpha_r} - \alpha_r) L_m}{\mu p \lambda_{ref}^2} (s + b)]$$

$$d(s) = (s+b)[(s+\alpha_r)^2 + (\frac{\alpha_r L_m \bar{i}_q}{\lambda_{ref}})^2] + \frac{\mu p \lambda_{ref}^2}{L_m} (s+\alpha_r - \frac{\alpha_r L_m^2 \bar{i}_q^2}{\lambda_{ref}^2})$$

It can be seen that the product  $\omega_c i_q$  plays an important role in the control design. When  $\omega_c i_q = 0$ , G(s) has a zero at the origin. Hence, it is impossible to design any controller with the integral action. This follows from the well known theory of servomechanisms [3]. When  $\omega_c i_q < 0$ , G(s) has a real zero in the right-half s-plane; hence, it is non-minimum phase. It is possible to design a controller with integral action to stabilize the system, but such a controller cannot be a PI controller. This fact can be seen by sketching the root locus of the system for different possible polezero patterns. For a PI controller, the root locus will always have a branch on the positive real axis. This leaves us with the case when  $\omega_c i_q$  is positive. In this case, the transfer function G(s) is minimum phase and we can design a PI controller with high-gain feedback to stabilize the closed-loop system and achieve good tracking properties. Such PI controller takes the form

$$I_q = \frac{(K_{wp}s + K_{wi})}{s} [\omega_{ref} - \Omega]$$

The condition

$$\omega_{c}\bar{i}_{q} = \bar{i}_{q} \left[ p \omega_{ref} + \frac{\hat{\alpha_{r}} L_{m}\bar{i}_{q}}{\lambda_{ref}} \right] > 0$$

is satisfied when the motor is operated in the motoring or braking modes, but not in the generating mode. A similar condition has also been presented in [2].

The condition  $\omega_c \bar{i}_q = 0$  is satisfied if  $\bar{i}_q = 0$  or  $\omega_c = 0$  [8]. The case  $\omega_c = 0$  indicates operation at zero frequency, in a braking mode corresponding to certain speed and torque. It is well known in the induction motor literature that operating the motor at zero (or low) frequency is challenging, and that a design for such case will have to exploit secondary phenomena of the machine, not conveyed in the machine model (3.1)-(3.3). The case  $\bar{i}_q = 0$ , regardless of the speed, indicates that the power

into the machine is negative.

Figure 3.1 presents a schematic for sensorless control of an induction motor using flux and speed observers. Three-phase stator currents are first transformed

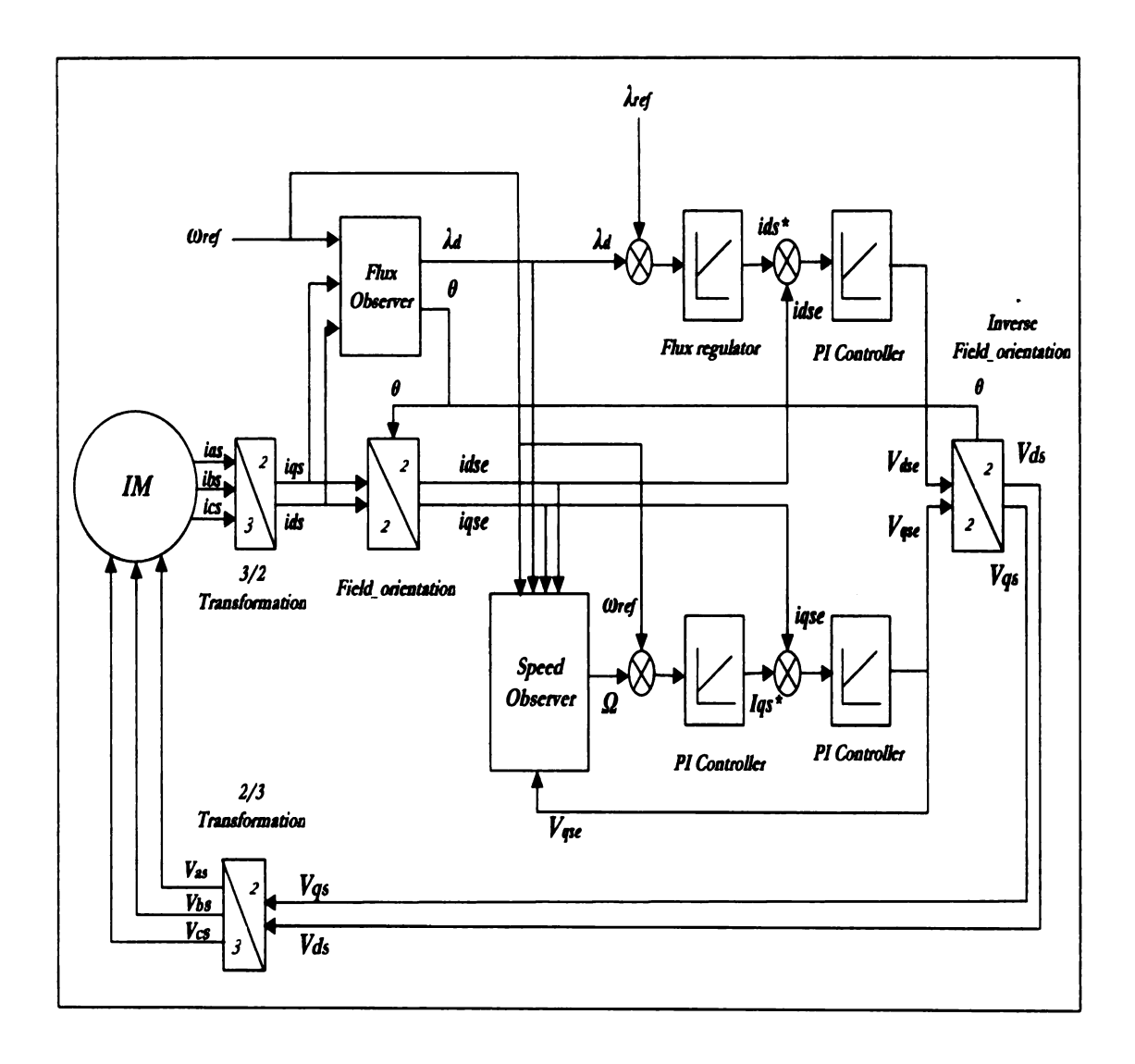


Figure 3.1. Sensorless control of an induction motor using traditional PI controllers

to d-q currents. The flux observer provides the flux estimate  $\lambda_d$  and angle  $\theta$ , for field-orientation, using these d-q currents and reference speed  $\omega_{ref}$ . The d-q currents are then transformed into field-coordinates. The speed Observer utilizes these field currents to provide a speed estimate. Two PI controllers are used for flux regulation and regulation of the d-axis current. For the speed regulation, a PI controller is used that regulates the q-axis current to its command. The voltage signals provided by the PI controllers are transformed back to original coordinates by inverse field-orientation and d-q to three-phase transformation.

# CHAPTER 4

# Speed Control Using Sliding Mode Control Strategy

#### 4.1 Introduction

The complex nonlinear nature of the induction motor model together with the fact that certain important quantities are not measured, present difficulties in designing the high performance induction machine drive control algorithms. In addition, the uncertainties pertaining to the imperfect knowledge of the system inputs and disturbances together with the inaccuracies in the machine modeling contribute to performance degradation of the feedback control system. Sliding mode control is a popular technique in nonlinear feedback control that operates effectively over a range of system parameter variations and disturbances.

Sliding mode control deals with robust control under the matching conditions; that is, when uncertain terms enter the state equation at the same point as the control input. In sliding mode control, the trajectories are forced to reach a sliding manifold in finite time and to stay on the manifold for all the future time. Motion on the manifold is independent of matched uncertainties. Its two main advantages are

- The dynamic behavior of the system may be tailored by the particular choice of switching function
- The closed-loop response becomes totally insensitive to a particular class of uncertainty related to the system parameter variations and disturbances.

By using a lower order model of the system, the sliding manifold is designed to achieve the control objective .

#### 4.1.1 Sliding Mode Control

Consider the system

$$\dot{x} = f(x) + g(x)u$$

$$y = h(x)$$

The sliding mode control law for such a system takes the form

$$u = -\beta(x)sgn(s)$$

where  $\beta(x)$  is bounded up and below by certain inequalities in order to satisfy the conditions for maintaining the motion on the sliding manifold and

$$sgn(s) = \begin{cases} 1, & s > 0 \\ -1, & s < 0. \end{cases}$$

The motion consists of a reaching phase during which the trajectories starting off the manifold s = 0 move towards it and reach it in finite time, followed by a sliding phase during which the motion is confined to the manifold s = 0 and the dynamics of the system are represented by the reduced order model of the system[7]. The manifold s = 0 is called the sliding manifold. A sketch of the typical phase portrait for a second-order system is shown in Figure 4.1.

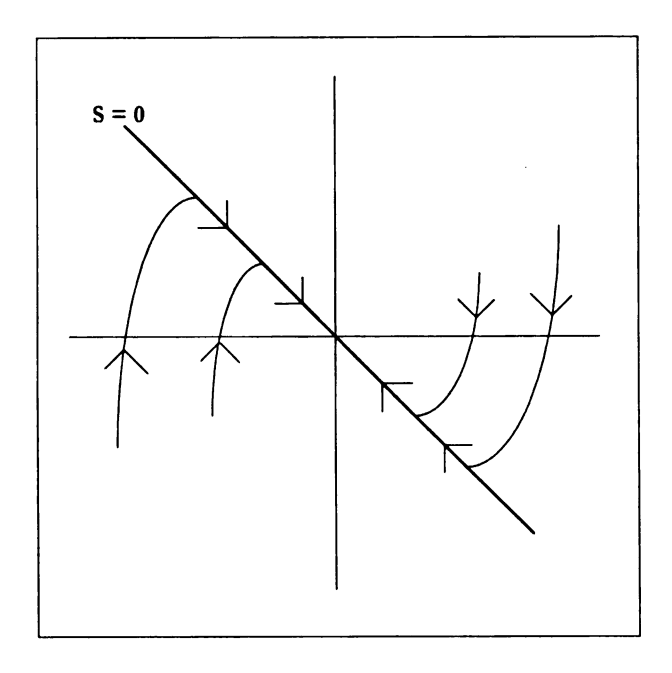


Figure 4.1. A typical phase portrait under sliding mode control

Due to the imperfections in switching devices and delays, the sliding mode control suffers from *chattering*. Two different approaches for reducing or eliminating chattering arc[7]

- Dividing the control into continuous and switching components so as to reduce the amplitude of the switchin component
- Replacing the signum sgn function by a high-slope saturation function

Using the second approach, the control law is taken as

$$u = -\beta(x)sat(s/\varepsilon)$$

where sat(.) is the saturation function defined by

$$sat(y) = \begin{cases} y, & \text{if } |y| \leq 1 \\ sgn(y), & \text{if } |y| > 1 \end{cases}$$

and  $\varepsilon$  is a positive constant. The slope of linear portion of  $sat(s/\varepsilon)$  is  $(1/\varepsilon)$ . A good approximation requires  $\varepsilon$  to be of a very small numerical value. In the limit, as  $\varepsilon \to 0$ , the saturation function  $sat(s/\varepsilon)$  approaches the signum function sgn(s).

# 4.1.2 Zero Dynamics and the Relative Degree of Nonlinear Systems

From the view point of designing feedback control for a nonlinear system, it is necessary to investigate certain important properties of the system. The two important properties of a nonlinear system considered here are the *relative degree* and the *zero dynamics*.

Relative degree of a nonlinear system is the number of derivatives of the output needed to make the input explicit for the system. The same term is used for a linear system in a context that it is the excess of poles over zeroes for the transfer function of a given linear system.

Zero dynamics of a nonlinear system represent the *internal dynamics* of the system when the output is identically zero. In linear systems, this matches nicely with the dynamic equations whose eigenvalues are the zeroes of the transfer function of linear system. This is critical for linear controller design because at high-gain the closed-loop poles migrate to open-loop zeros and these zeros determine the boundedness of the control required for linear tracking. Zero dynamics are important for many nonlinear controller design procedures like feedback linearization, sliding mode control and adaptive control. Details of zero dynamics matter because if the system possess unstable zero dynamics, it can invalidate many control design procedures. Theoretical foundation of the calculation of the relative degree and the zero dynamics is given in [7, 5].

Consider a single-input single-output nonlinear system

$$\dot{x} = f(x) + g(x)u$$

$$y = h(x)$$

The calculation of the zero dynamics of this system consists of two steps

- Bring the system in a normal form with a nonlinear invertible change of coordinates  $z = \Phi(x)$
- Extract the zero dynamics equations from this form

First, calculate r components of  $\Phi$  as

$$\begin{array}{rcl} \phi_1(x) & = & h(x) \\ \\ \phi_2(x) & = & L_f h(x) \\ \\ & \vdots \\ \\ \phi_r(x) & = & L_f^{r-1} h(x) \end{array}$$

where  $L_f h(x) = \frac{\partial h(x)}{\partial x} f(x)$  and  $L_f^2 h(x)$  etc. are recursively defined and r is the relative degree i.e. the smallest r for which  $L_g L_f^{r-1} h(x) \neq 0$ , with  $L_g = \frac{\partial (.)}{\partial x} g(x)$ . Choose the remaining n-r new coordinates  $z_i$ , i=r+1,...,n so that  $\Phi(x)$  is invertible at  $x=x_0$ . Additionally, select  $\phi_i$ , i=r+1,...,n so that [5]

$$L_{q}z_{i}=L_{q}\phi_{i}(x)=0$$

The normal form in the new coordinates z is then

$$\dot{z}_1 = z_2$$

and

$$y = z_1$$

where  $b(x) = L_f^r h(x)$ ,  $a(x) = L_g L_f^{r-1} h(x)$  and  $q_i(x) = L_f \phi_i(x)$ , i = r+1, ..., n. We use the relation

$$x = \Phi^{-1}(z)$$

to express b(x), a(x) and  $q_i(x)$  as functions of z.

The above equations represent the system in the *normal form*. This form decomposes the system into an external part and an internal part. In order to obtain y=0, we choose the input u as -b(z)/a(z) and the initial conditions  $x_0$  such that  $z_i=0, i=1,...,r$ . By definition, the zero dynamics of the system are then given by the equations for  $\dot{z}_{r+1},...,\dot{z}_n$ , with the coordinates  $z_1,...,z_r$  set to zero. With

$$\xi = [z_1, ..., z_r]^T$$

$$\eta = [z_{r+1}, ..., z_n]^T$$

the last (n-r) equations of the normal form can be written as

$$\dot{\eta} = q(\xi, \eta)$$

and the zero dynamics are obtained by setting  $\xi = 0$ :

$$\dot{\eta} = q(0,\eta)$$

# 4.1.3 Regulation via Integral Control in Relative Degree-1 Systems

Suppose the system

$$\dot{x} = f(x) + g(x)u$$

$$y = h(x)$$

has relative degree 1 for all x in a domain  $D \subset \mathbb{R}^n$ . Our goal is to design a state feedback control law such that the output y asymptotically tracks a constant reference signal r. When the signum function  $\operatorname{sgn}(s)$  is approximated by the saturation function  $\operatorname{sat}(s/\varepsilon)$ , the regulation error will be ultimately bounded by a constant  $k\varepsilon$  for some k>0. Using an integral control provides zero steady-state error, therefore, we augment the integral of the regulation error y-r with the system and design a feedback controller that stabilizes the augmented system at an equilibrium point, say  $x_{ss}$ , where y=r. We use the integrator

$$\dot{\sigma} = y - r = e$$

with the system equations to obtain the augmented system

$$\dot{x} = f(x) + g(x)u$$

$$\dot{\sigma} = e = y - r$$

To proceed with the design of the sliding mode control, we can take,

$$s = k_0 \sigma + e$$

where  $k_0$  is a positive constant. The sliding mode control law for such a system takes the form

$$u = -\beta(x)sat(s/\varepsilon)$$

# 4.2 Sliding Mode Controller Design For the Induction Motor

In order to proceed with designing the speed controller based on the sliding mode control theory, the reduced-order machine model (3.20)-(3.23) is considered. To this effect, the *error functions* can be defined as

$$e = \omega - \omega_{ref}$$

$$y = \Omega - \omega_{ref}$$

and the equations (3.20)-(3.23) can be rewritten as

$$\dot{e_d} = -\alpha_r e_d + (-pe + \hat{\alpha_r} L_m i_q / \lambda_{ref}) e_q \tag{4.1}$$

$$\dot{e_q} = -(-pe + \hat{\alpha_r} L_m i_q / \lambda_{ref}) e_d - \alpha_r e_q + (\hat{\alpha_r} - \alpha_r) L_m i_q - pe \lambda_{ref}$$
(4.2)

$$\dot{e} = \mu[i_q(\lambda_{ref} - e_d) + \frac{\lambda_{ref}}{L_m}e_q] - be - b\omega_{ref} - T_L/m - \dot{\omega}_{ref}$$
(4.3)

$$y = \left(\frac{\lambda_{ref} - e_d}{\lambda_{ref}}\right)e - \frac{\omega_{ref}}{\lambda_{ref}}e_d + \frac{\alpha_r}{p\lambda_{ref}}e_q - ai_q \tag{4.4}$$

where

$$a = \frac{(\hat{\alpha_s} - \alpha_s)\eta + (\hat{\alpha_r} - \alpha_r)\beta L_m}{\beta p \lambda_{ref}}$$

The system is single-input-single-output where  $e_d$ ,  $e_q$  and e are the three states, the q-axis current is the control input and a speed estimate  $\Omega$  (provided by a high-gain observer) is the measured output. The error functions have been introduced to conveniently proceed with the analysis.

The goal here is to address the speed regulation via integral control based on the sliding mode control theory, such that the rotor speed  $\omega$  asymptotically tracks a bounded time-varying reference speed  $\omega_{ref}$ . Clearly, the equilibrium point of interest pertaining to the reduced order system would be such that the flux estimation errors  $e_d$  and  $e_q$ , and the speed error e are zero. The following section presents the analysis related to the asymptotic stability of the desired equilibrium point.

#### 4.2.1 Zero Dynamics of the system

For the purpose of stability analysis, the nominal parameters case is considered when  $\hat{R_r} = R_r$  and  $\hat{R_s} = R_s$ , which makes a = 0 in equation (4.4). The resulting system has a relative degree 1 in  $\mathbb{R}^3$  as the control input appears in the output equation upon calculating the first derivative of the output. The internal (or zero) dynamics of the system are described by equations (4.1) and (4.2) when y is set identically zero. The external dynamics of the system are described by equation (4.3). Analysis of the zero dynamics provides insight into the asymptotic stability of the origin. The system is said to be minimum phase if the origin of the zero dynamics is asymptotically stable [7]. When

$$y \equiv 0$$

in equation (4.4); we obtain

$$\epsilon = \frac{\omega_{ref} e_d - \frac{\alpha_r}{p} e_q}{\lambda_{ref} - e_d} \tag{4.5}$$

Taking the time derivative of the preceding equation

$$\dot{e} = \frac{\partial}{\partial e_d} \left[ \frac{\omega_{ref} e_d - \frac{\alpha_r}{p} e_q}{\lambda_{ref} - e_d} \right] \dot{e_d} + \frac{\partial}{\partial e_d} \left[ \frac{\omega_{ref} e_d - \frac{\alpha_r}{p} e_q}{\lambda_{ref} - e_d} \right] \dot{e_q}$$

and substituting the values of  $\dot{e_d}$  and  $\dot{e_q}$  from equations (4.1) and (4.2), we obtain

$$\begin{split} \dot{e} &= \frac{1}{(\lambda_{ref} - e_d)} \Biggl\{ -\alpha_r \omega_{ref} e_d - pe\omega_{ref} e_q + (\alpha_r L_m i_q / \lambda_{ref}) \omega_{ref} e_q \\ &- \alpha_r e e_d + \frac{\frac{\alpha_r^2}{p} L_m i_q e_d}{\lambda_{ref}} + \frac{\alpha_r^2}{p} e_q + \alpha_r e \lambda_{ref} \Biggr\} \\ &+ \frac{1}{(\lambda_{ref} - e_d)^2} \Biggl\{ -\alpha_r \omega_{ref} e_d^2 + \Bigl[ \frac{\alpha_r^2}{p} - pe\omega_{ref} + (\alpha_r L_m i_q / \lambda_{ref}) \omega_{ref} \Bigr] e_d e_q \\ &+ \Bigl[ \alpha_r e - \frac{\frac{\alpha_r^2}{p} L_m i_q}{\lambda_{ref}} \Bigr] e_q^2 \Biggr\} \end{split}$$

The second order terms in  $e_d$  and  $e_q$  that appear in the above relationship can be approximated by  $O(\|e_f\|^2)$ , where  $\|e_f\|^2 = e_d^2 + e_q^2$ . Further, substituting the value of  $e_q$  from equation (4.5); we obtain

$$\dot{e} = \frac{1}{(\lambda_{ref} - e_d)} \left\{ \left( -\alpha_r \omega_{ref} + \frac{\frac{\alpha_r^2}{p} L_m i_q}{\lambda_{ref}} \right) e_d + \left( \frac{\alpha_r^2}{p} + \alpha_r L_m i_q \omega_{ref} / \lambda_{ref} \right) e_q + \frac{\lambda_{ref}}{(\lambda_{ref} - e_d)} \left[ \alpha_r \omega_{ref} e_d - \frac{\alpha_r}{p} e_q \right] \right\} + O(\|e_f\|^2)$$

or.

$$\dot{e} = \frac{1}{(\lambda_{ref} - e_d)} \left[ -\alpha_r \omega_{ref} e_d + \frac{\alpha_r^2}{p} e_q + \frac{\lambda_{ref}}{(\lambda_{ref} - e_d)} (\alpha_r \omega_{ref} e_d - \frac{\alpha_r}{p} e_q) \right]$$

$$+ \frac{1}{\lambda_{ref} (\lambda_{ref} - e_d)} \left( \frac{\alpha_r^2}{p} L_m e_d + \alpha_r \omega_{ref} L_m e_q \right) i_q$$

$$+ O(\|e_f\|^2)$$

$$(4.6)$$

Similarly, substituting the value of e from equation (4.5) in equation (4.3) we get

$$\dot{e} = \mu(\lambda_{ref} - e_d)i_q - \frac{b\omega_{ref}}{(\lambda_{ref} - e_d)}e_d + \left(\frac{\mu\lambda_{ref}}{L_m} + \frac{b\alpha_r}{p(\lambda_{ref} - e_d)}\right)e_q - (b\omega_{ref} + \frac{T_L}{m} + \dot{\omega}_{ref})$$

$$(4.7)$$

Comparing equations (4.6) and (4.7); we have

$$\begin{split} \left\{ \mu(\lambda_{ref} - e_d) - \frac{1}{\lambda_{ref}(\lambda_{ref} - e_d)} \left( \frac{\alpha_r^2}{p} L_m e_d + \alpha_r \omega_{ref} L_m e_q \right) \right\} i_q \\ = \frac{1}{(\lambda_{ref} - e_d)} \left[ -\alpha_r \omega_{ref} e_d + \frac{\alpha_r^2}{p} e_q + \frac{\lambda_{ref}}{(\lambda_{ref} - e_d)} \left( \alpha_r \omega_{ref} e_d - \frac{\alpha_r}{p} e_q \right) \right. \\ \left. + b \omega_{ref} e_d - \frac{b \alpha_r}{p} e_q \right] - \frac{\mu \lambda_{ref}}{L_m} e_q + \left( b \omega_{ref} + \frac{T_L}{m} + \dot{\omega}_{ref} \right) \end{split}$$

or

$$i_{q} = \frac{\lambda_{ref}}{\mu \lambda_{ref} (\lambda_{ref} - e_{d})^{2} - (\frac{\alpha_{r}^{2}}{p} L_{m} e_{d} + \alpha_{r} \omega_{ref} L_{m} e_{q})} \left\{ \left[ (b - \alpha_{r}) \omega_{ref} + \frac{\alpha_{r} \omega_{ref} \lambda_{ref}}{(\lambda_{ref} - e_{d})} \right] e_{d} + \left[ \frac{-\alpha_{r}}{p} (b - \alpha_{r}) - \frac{\frac{\alpha_{r}}{p} \lambda_{ref}}{(\lambda_{ref} - e_{d})} - \frac{\mu (\lambda_{ref} - e_{d}) \lambda_{ref}}{L_{m}} \right] e_{q} + \left[ (\lambda_{ref} - e_{d}) (b \omega_{ref} + \frac{T_{L}}{m} + \dot{\omega}_{ref}) \right] \right\} + O(\|e_{f}\|^{2})$$

$$(4.8)$$

The next steps involve substituting the value of  $i_q$  from (4.8) into (4.1) and (4.2) to obtain the equations for the zero dynamics of the system. Towards that end, we substitute the value of  $i_q$  in (4.1) and after some simplifications, we obtain;

$$\frac{e_{d}}{e_{d}} = -\alpha_{r}e_{d} + \frac{\alpha_{r}L_{m}e_{q}}{\mu\lambda_{ref}(\lambda_{ref} - e_{d})^{2} - \frac{\alpha_{r}^{2}}{p}L_{m}e_{d} - \alpha_{r}\omega_{ref}L_{m}e_{q}} \left\{ \left[ (b - \alpha_{r})\omega_{ref} + \frac{\alpha_{r}\omega_{ref}\lambda_{ref}}{(\lambda_{ref} - e_{d})} \right] e_{d} + \left[ \frac{-\alpha_{r}}{p}(b - \alpha_{r}) - \frac{\frac{\alpha_{r}}{p}\lambda_{ref}}{(\lambda_{ref} - e_{d})} - \frac{\mu(\lambda_{ref} - e_{d})\lambda_{ref}}{L_{m}} \right] e_{q} + \left[ (\lambda_{ref} - e_{d})(b\omega_{ref} + \frac{T_{L}}{m} + \dot{\omega}_{ref}) \right] \right\} + O(\|e_{f}\|^{2}) \tag{4.9}$$

Similarly when we substitute the value of iq in equation (4.2), we obtain

$$\dot{e_q} = \frac{-\alpha_r L_m e_d}{\mu \lambda_{ref} (\lambda_{ref} - e_d)^2 - \frac{\alpha_r^2}{p} L_m e_d - \alpha_r \omega_{ref} L_m e_q} \left\{ \left[ (b - \alpha_r) \omega_{ref} + \frac{\alpha_r \omega_{ref} \lambda_{ref}}{(\lambda_{ref} - e_d)} \right] e_d + \left[ \frac{-\alpha_r}{p} (b - \alpha_r) - \frac{\frac{\alpha_r}{p} \lambda_{ref}}{(\lambda_{ref} - e_d)} - \frac{\mu (\lambda_{ref} - e_d) \lambda_{ref}}{L_m} \right] e_q + \left[ (\lambda_{ref} - e_d) (b \omega_{ref} + \frac{T_L}{m} + \dot{\omega}_{ref}) \right] \right\} - \alpha_r e_q - \frac{\lambda_{ref}}{(\lambda_{ref} - e_d)} \left( p \omega_{ref} e_d - \alpha_r e_q \right) + O(\|e_f\|^2) \tag{4.10}$$

A further approximation of the second-order terms in  $e_d$  and  $e_q$  simplifies the equations (4.9) and (4.10) to

$$\dot{\epsilon_d} = -\alpha_r e_d + \frac{\alpha_r L_m}{\mu \lambda_{ref}^2} \left( b\omega_{ref} + \frac{T_L}{m} + \dot{\omega}_{ref} \right) \epsilon_q + O(\|e_f\|^2)$$
(4.11)

$$\dot{e_q} = -\left[p\omega_{ref} + \frac{\alpha_r L_m}{\mu \lambda_{ref}^2} \left(b\omega_{ref} + \frac{T_L}{m} + \dot{\omega}_{ref}\right)\right] e_d + O(\|e_f\|^2)$$
(4.12)

Assuming that  $\omega_{ref}(t)$  and  $T_L(t)$  approach constant limits as  $t \to \infty$ , i.e.  $\lim_{t\to\infty}\omega_{ref}(t) = \bar{\omega}_{ref}$ ,  $\lim_{t\to\infty}\dot{\omega}_{ref}(t) = 0$ ,  $\lim_{t\to\infty}T_L(t) = \bar{T}_L$ , and neglecting the second-order terms in  $\epsilon_d$  and  $\epsilon_q$ , equations (4.11) and (4.12) constitute a linear time-varying system of the form

$$\dot{x} = [A + B(t)]x$$

where

$$A = \begin{pmatrix} -\alpha_r & \frac{\alpha_r L_m}{\mu \lambda_{ref}^2} (b\bar{\omega}_{ref} + \frac{\bar{T}_L}{m}) \\ -p\bar{\omega}_{ref} + \frac{\alpha_r L_m}{\mu \lambda_{ref}^2} (b\bar{\omega}_{ref} + \frac{\bar{T}_L}{m}) & 0 \end{pmatrix}$$

$$B(t) = \begin{pmatrix} 0 & \frac{\alpha_r L_m}{\mu \lambda_{ref}^2} \left[ b \tilde{\omega}_{ref} + \dot{\omega}_{ref} + \frac{\tilde{T}_L}{m} \right] \\ -p \tilde{\omega}_{ref} - \frac{\alpha_r L_m}{\mu \lambda_{ref}^2} \left[ b \tilde{\omega}_{ref} + \dot{\omega}_{ref} + \frac{\tilde{T}_L}{m} \right] & 0 \end{pmatrix}$$

where  $\tilde{\omega}_{ref} = \omega_{ref} - \bar{\omega}_{ref}$ ,  $\tilde{T}_L = T_L - \bar{T}_L$ , A is constant and B(t) is time-varying such that  $\lim_{t\to\infty} B(t) = 0$ .

The above system can be viewed as a perturbed system where A is the system matrix of the nominal linear system and B(t) is the perturbation term. Theory of stability of perturbed systems [7, Example: 9.6] proves that if the origin is an exponentially stable equilibrium point of the nominal system

$$\dot{x} = Ax$$

and if

$$B(t) \to 0$$
 as  $t \to \infty$ 

then the origin is a globally exponentially stable equilibrium point of the perturbed system  $\dot{x} = [A + B(t)]x$ .

In order to investigate the stability of the origin  $(e_d = e_q = 0)$  as an asymptotically stable equilibrium point for the system (4.11)-(4.12), we proceed with the calculation of the eigenvalues of the matrix A.

$$A = \begin{pmatrix} -\alpha_r & \frac{\alpha_r L_m}{\mu \lambda_{ref}^2} (b\bar{\omega}_{ref} + \frac{\bar{T}_L}{m}) \\ -p\bar{\omega}_{ref} - \frac{\alpha_r L_m}{\mu \lambda_{ref}^2} (b\bar{\omega}_{ref} + \frac{\bar{T}_L}{m}) & 0 \end{pmatrix}$$

$$\lambda I - A = \begin{pmatrix} \lambda + \alpha_r & \frac{-\alpha_r L_m}{\mu \lambda_{ref}^2} (b \bar{\omega}_{ref} + \frac{\bar{T}_L}{m}) \\ p \bar{\omega}_{ref} + \frac{\alpha_r L_m}{\mu \lambda_{ref}^2} (b \bar{\omega}_{ref} + \frac{\bar{T}_L}{m})] & \lambda \end{pmatrix}$$

which gives

$$\left|\lambda I - A\right| = \lambda(\lambda + \alpha_r) + \left[p\bar{\omega}_{ref} + \frac{\alpha_r L_m}{\mu \lambda_{ref}^2} (b\bar{\omega}_{ref} + \frac{\bar{T}_L}{m})\right] \left[\frac{\alpha_r L_m}{\mu \lambda_{ref}^2} (b\bar{\omega}_{ref} + \frac{\bar{T}_L}{m})\right]$$

or

$$\left|\lambda I - A\right| = \lambda^2 + \alpha_r \lambda + \left[p\bar{\omega}_{ref}\kappa + \kappa^2\right]$$

where

$$\kappa = \frac{\alpha_r L_m}{\mu \lambda_{ref}^2} (b \bar{\omega}_{ref} + \frac{\bar{T}_L}{m})$$

The eigenvalues of A

$$\lambda_{1,2} = -\tfrac{\alpha_r}{2} \pm \tfrac{1}{2} \sqrt{\alpha_r^2 - 4 \left[ p \bar{\omega}_{ref} \kappa + \kappa^2 \right]}$$

have negative real parts only when the product  $\kappa(p\bar{\omega}_{ref}+\kappa)>0$ , which is the case when the steady-state speed command  $\bar{\omega}_{ref}$  and the steady-state load torque  $\bar{T}_L$  both have the same sign, positive or negative. This condition is similar to the one obtained in the previous work [8], referred to in Chapter 3, where the product  $\bar{\omega}_{ciq}$  determines a similar stability condition. The condition  $\kappa(p\bar{\omega}_{ref}+\kappa)>0$  is satisfied when the motor is operated in the motoring or braking modes only. If the motor is operated in the generating mode the stability condition is violated as the product  $\kappa(p\bar{\omega}_{ref}+\kappa)$  is no longer a positive term.

### 4.2.2 Speed Regulation via Integral Control

A sliding mode controller with integral action is designed in order to address the speed regulation problem. Using integral control provides zero steady-state error. Therefore, we augment the integral of the regulation error with the system and design a feedback controller that stabilizes the augmented system at the desired equilibrium point. Consider the reduced-order machine model (3.20)-(3.23) with the error

functions defined as

$$e = \omega - \omega_{ref}$$

$$y = \Omega - \omega_{ref}$$

In the nominal case  $\hat{\alpha}_r = \alpha_r$ ,  $\hat{\alpha}_s = \alpha_s$ , equations (3.20)-(3.23) can be rewritten as

$$\dot{e_d} = -\alpha_r e_d + (-pe + \alpha_r L_m i_q / \lambda_{ref}) e_q \tag{4.13}$$

$$\dot{e_q} = -(-pe + \alpha_r L_m i_q / \lambda_{ref}) e_d - \alpha_r e_q - pe \lambda_{ref}$$
(4.14)

$$\dot{e} = \mu[i_q(\lambda_{ref} - e_d) + \frac{\lambda_{ref}}{L_m}e_q] - be - b\omega_{ref} - T_L/m - \dot{\omega}_{ref}$$
 (4.15)

$$y = \left(\frac{\lambda_{ref} - e_d}{\lambda_{ref}}\right)e - \frac{\omega_{ref}}{\lambda_{ref}}e_d + \frac{\alpha_r}{p\lambda_{ref}}e_q \tag{4.16}$$

The system is single-input-single-output with  $e_d$ ,  $e_q$  and e as the states, the q-axis current as the control input and the speed estimate  $\Omega$  (provided by a high-gain observer) as the measured output. Augment the integrator

$$\dot{\sigma} = y$$

$$= \Omega - \omega_{ref} \tag{4.17}$$

with the system (4.13)-(4.16), and take

$$s = k_0 \sigma + y \tag{4.18}$$

where  $k_0$  is a positive constant. The continuous sliding mode control law for the system is

$$i_q = -Ksat(s/\varepsilon) \tag{4.19}$$

where K should be chosen to satisfy the condition

$$s\dot{s} < 0 \tag{4.20}$$

outside the boundary layer  $\{|s| \le \varepsilon\}$  to ensure that the trajectories reach the boundary layer in finite time and stay inside thereafter.

Substituting the value of y from equation (4.16) in equation (4.18) yields

$$s = k_0 \sigma + \left(\frac{\lambda_{ref} - e_d}{\lambda_{ref}}\right) e - \frac{\omega_{ref}}{\lambda_{ref}} e_d + \frac{\alpha_r}{p \lambda_{ref}} e_q$$

$$\dot{s} = k_0 \dot{\sigma} + \left(\frac{\lambda_{ref} - e_d}{\lambda_{ref}}\right) \dot{e} - \frac{e}{\lambda_{ref}} \dot{e_d} - \frac{\omega_{ref}}{\lambda_{ref}} \dot{e_d} + \frac{\alpha_r}{p\lambda_{ref}} \dot{e_q}$$

Substituting the values of  $\dot{e_d}$ ,  $\dot{e_q}$ ,  $\dot{e}$  and  $\dot{\sigma}$  from equations (4.13)-(4.15) and (4.17), we obtain

$$\begin{split} \dot{s} &= k_0 y \\ &+ \Big(\frac{\lambda_{ref} - e_d}{\lambda_{ref}}\Big) \Big\{ \mu [i_q (\lambda_{ref} - e_d) + \frac{\lambda_{ref}}{L_m} e_q] - be - b\omega_{ref} - T_L/m - \dot{\omega}_{ref} \Big\} \\ &- \frac{e}{\lambda_{ref}} \Big\{ - \alpha_r e_d + (-pe + \alpha_r L_m i_q/\lambda_{ref}) e_q \Big\} \\ &- \frac{\omega_{ref}}{\lambda_{ref}} \Big\{ - \alpha_r e_d + (-pe + \alpha_r L_m i_q/\lambda_{ref}) e_q \Big\} \\ &+ \frac{\alpha_r}{p\lambda_{ref}} \Big\{ - (-pe + \alpha_r L_m i_q/\lambda_{ref}) e_d - \alpha_r e_q - pe\lambda_{ref} \Big\} \end{split}$$

which simplifies to

$$\begin{split} \dot{s} &= \left\{ \frac{\alpha_r}{\lambda_{ref}} \Big( 2e + \omega_{ref} \Big) e_d + \Big( \frac{pe(e + \omega_{ref})}{\lambda_{ref}} + \frac{\mu}{L_m} (\lambda_{ref} - e_d) - \frac{\alpha_r^2}{p\lambda_{ref}} \Big) e_q \\ &- \Big( \frac{b(\lambda_{ref} - e_d) + \alpha_r \lambda_{ref}}{\lambda_{ref}} \Big) e + k_0 y \\ &- \Big( \frac{\lambda_{ref} - e_d}{\lambda_{ref}} \Big) \Big( b\omega_{ref} + T_L/m + \dot{\omega}_{ref} \Big) \right\} \end{split}$$

$$+ \left\{ \frac{\mu (\lambda_{ref} - e_d)^2}{\lambda_{ref}} - \frac{\alpha_r L_m (e + \omega_{ref}) e_q}{\lambda_{ref}^2} - \frac{\alpha_r^2 L_m}{p \lambda_{ref}^2} e_d \right\} i_q$$

The above expression can be written in the form

$$\dot{s} = F + Gi_q \tag{4.21}$$

where

$$F = \left\{ \frac{\alpha_r}{\lambda_{ref}} \left( 2e + \omega_{ref} \right) e_d + \left( \frac{pe(e + \omega_{ref})}{\lambda_{ref}} + \frac{\mu}{L_m} (\lambda_{ref} - e_d) - \frac{\alpha_r^2}{p\lambda_{ref}} \right) e_q - \left( \frac{b(\lambda_{ref} - e_d) + \alpha_r \lambda_{ref}}{\lambda_{ref}} \right) e + k_0 y - \left( \frac{\lambda_{ref} - e_d}{\lambda_{ref}} (b\omega_{ref} + T_L/m + \dot{\omega}_{ref}) \right) \right\}$$

$$G = \left\{ \frac{\mu (\lambda_{ref} - e_d)^2}{\lambda_{ref}} - \frac{\alpha_r L_m (e + \omega_{ref}) e_q}{\lambda_{ref}^2} - \frac{\alpha_r^2 L_m}{p \lambda_{ref}^2} e_d \right\}$$
(4.22)

The function G should satisfy the condition

$$G \ge G_0 > 0 \tag{4.23}$$

for some positive constant  $G_0$ , which is the case in the neighborhood of  $\epsilon_d=\epsilon_q=0$ .

From (4.21),

$$s\dot{s} = sF + sGi_q \tag{4.24}$$

For  $|s| \ge \varepsilon$ , the sliding mode control (4.19) takes the form

$$i_q = -Ksgn(s)$$

and equation (4.24) can be written as

$$s\dot{s} = sF - GK|s|$$

$$= G\frac{sF}{G} - GK|s|$$

$$\leq G|s|\left|\frac{F}{G}\right| - GK|s|$$

We assume that the ratio  $\left| rac{F}{G} \right|$  satisfies the inequality

$$\left|\frac{F}{G}\right| \le K - K_0 \tag{4.25}$$

where  $K_0$  is a positive constant. Then,

$$s\dot{s} \leq G|s|(K - K_0) - GK|s|$$

$$= -K_0G|s|$$

$$\leq -K_0G_0|s| \qquad (4.26)$$

It is clear from the foregoing analysis that inequalities (4.23) and (4.25), rewritten as

$$K \geq K_0 + \left| \frac{F}{G} \right|$$

$$G \geq G_0 > 0 \tag{4.27}$$

should hold over the domain of interest in order to ensure that all trajectories outside the boundary layer  $\{|s| \le \varepsilon\}$  reach it in finite time and those inside the boundary layer cannot leave, as portrayed in Figure 4.2.

In order to analyze the system inside the boundary layer, consider

$$\dot{e_d} = -\alpha_r e_d + (-pe + \alpha_r L_m i_q / \lambda_{ref}) e_q \tag{4.28}$$

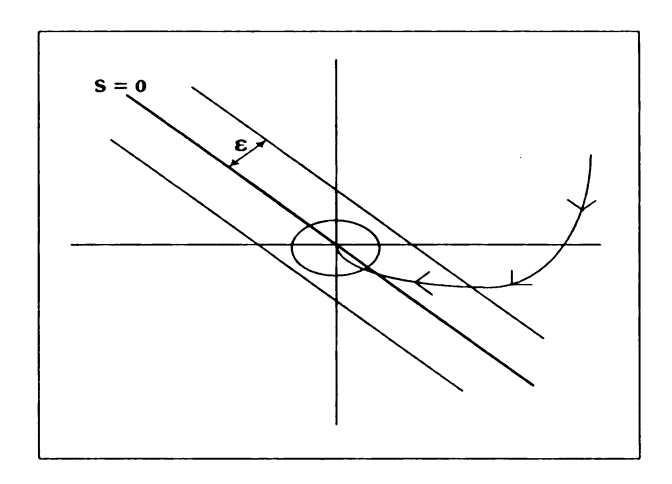


Figure 4.2. Trajectory outside the boundary layer reach it in finite time and stay inside thereafter

$$\dot{e_q} = -(-pe + \alpha_r L_m i_q / \lambda_{ref}) e_d - \alpha_r e_q - pe \lambda_{ref}$$
(4.29)

$$\dot{e} = \mu[i_q(\lambda_{ref} - e_d) + \frac{\lambda_{ref}}{L_m}e_q] - be - b\omega_{ref} - T_L/m - \dot{\omega}_{ref}$$
 (4.30)

$$\dot{\sigma} = -k_0 \sigma + s \tag{4.31}$$

$$y = \left(\frac{\lambda_{ref} - e_d}{\lambda_{ref}}\right) e - \frac{\omega_{ref}}{\lambda_{ref}} e_d + \frac{\alpha_r}{p\lambda_{ref}} e_q$$
 (4.32)

$$s = k_0 \sigma + y \tag{4.33}$$

Inside the boundary layer, the control input (4.19) is given by

$$i_q = -K(s/\varepsilon) \tag{4.34}$$

Substituting the value of s from equation (4.33), we obtain

$$i_{q} = \frac{-K}{\varepsilon} \left[ k_{o}\sigma + \left( \frac{\lambda_{ref} - e_{d}}{\lambda_{ref}} \right) e - \frac{\omega_{ref}}{\lambda_{ref}} e_{d} + \frac{\alpha_{r}}{p\lambda_{ref}} e_{q} \right]$$
(4.35)

Substituting the value of  $i_q$  from equation (4.35) in equation (4.28) yields

$$\begin{array}{lcl} \dot{e_d} & = & -\alpha_r e_d - pee_q \\ & & - \left(\alpha_r L_m / \lambda_{ref}\right) \frac{K}{\varepsilon} \left[k_o \sigma + \left(\frac{\lambda_{ref} - e_d}{\lambda_{ref}}\right) e - \frac{\omega_{ref}}{\lambda_{ref}} e_d + \frac{\alpha_r}{p \lambda_{ref}} e_q\right] e_q \end{array}$$

Neglecting second-order terms in  $e_d$  and  $e_q$ , the above equation simplifies to

$$\dot{e_d} = -\alpha_r \epsilon_d - pee_q - \left(\alpha_r L_m / \lambda_{ref}\right) \frac{K}{\varepsilon} \left(k_o \sigma + e\right) e_q + O(\|\epsilon_f\|^2)$$
(4.36)

Substituting the value of  $i_q$  from equation (4.35) in equation (4.29), we obtain

$$\dot{e_q} = pee_d + \left(\alpha_r L_m / \lambda_{ref}\right) \frac{K}{\varepsilon} \left[k_o \sigma + \left(\frac{\lambda_{ref} - e_d}{\lambda_{ref}}\right) e - \frac{\omega_{ref}}{\lambda_{ref}} e_d + \frac{\alpha_r}{p \lambda_{ref}} e_q\right] e_d \\
- \alpha_r e_q - pe \lambda_{ref}$$

which simplifies to

$$\dot{e_q} = pee_d + \left(\alpha_r L_m / \lambda_{ref}\right) \frac{K}{\varepsilon} \left(k_o \sigma + e\right) e_d - \alpha_r e_q - pe \lambda_{ref} + O(\|e_f\|^2)$$
(4.37)

Similarly, substituting the value of  $i_q$  from equation (4.35) in equation (4.30) yields

$$\dot{e} = -\mu(\lambda_{ref} - e_d) \frac{K}{\varepsilon} \left[ k_o \sigma + \left( \frac{\lambda_{ref} - e_d}{\lambda_{ref}} \right) e - \frac{\omega_{ref}}{\lambda_{ref}} e_d + \frac{\alpha_r}{p \lambda_{ref}} e_q \right] + \frac{\mu \lambda_{ref}}{L_m} e_q - be - b\omega_{ref} - T_L/m - \dot{\omega}_{ref}$$

and this simplifies to

$$\begin{split} \dot{e} &= \frac{\mu K}{\varepsilon} \left( k_0 \sigma + \omega_{ref} \right) e_d + \mu \left( \frac{\lambda_{ref}}{L_m} - \frac{K \alpha_r / p}{\varepsilon} \right) e_q \\ &- \left( b + \mu \frac{K}{\varepsilon} \lambda_{ref} \right) e - \left( \mu \frac{K k_0}{\varepsilon} \lambda_{ref} \right) \sigma - \left( b \omega_{ref} + T_L / m + \dot{\omega}_{ref} \right) \end{split}$$

$$+ O(\|e_f\|^2) \tag{4.38}$$

Neglecting the the second-order terms in  $e_d$  and  $e_q$ , the system can be characterized by the fourth-order state model

$$\dot{e_d} = -\alpha_r e_d - pee_q - \left(\alpha_r L_m / \lambda_{ref}\right) \frac{K}{\epsilon} \left(k_o \sigma + e\right) e_q$$
 (4.39)

$$\dot{e_q} = pee_d + \left(\alpha_r L_m / \lambda_{ref}\right) \frac{K}{\varepsilon} \left(k_o \sigma + e\right) e_d - \alpha_r e_q - pe \lambda_{ref}$$
(4.40)

$$\dot{e} = \frac{\mu K}{\varepsilon} \left( k_0 \sigma + \omega_{ref} \right) e_d + \mu \left( \frac{\lambda_{ref}}{L_m} - \frac{K \alpha_r / p}{\varepsilon} \right) e_q - \left( b + \mu \frac{K}{\varepsilon} \lambda_{ref} \right) e_q$$

$$-\left(\mu \frac{Kk_0}{\varepsilon} \lambda_{ref}\right) \sigma - \left(b\omega_{ref} + T_L/m + \dot{\omega}_{ref}\right) \tag{4.41}$$

$$\dot{\sigma} = \left(\frac{\lambda_{ref} - e_d}{\lambda_{ref}}\right) e - \frac{\omega_{ref}}{\lambda_{ref}} e_d + \frac{\alpha_r}{p \lambda_{ref}} e_q \tag{4.42}$$

In order to analyze the performance of the system, inside the boundary layer, we examine the behavior of the system in the vicinity of the equilibrium point. Towards that end, we write the equilibrium equations under the steady-state conditions  $\omega_{ref} = \bar{\omega}_{ref}$ ,  $T_L = \bar{T}_L$  and  $\dot{\omega}_{ref} = 0$ .

$$0 = -\alpha_r \bar{e}_d - p\bar{e}\bar{e}_q - \left(\alpha_r L_m / \lambda_{ref}\right) \frac{K}{\varepsilon} \left(k_o \bar{\sigma} + \bar{e}\right) \bar{e}_q \tag{4.43}$$

$$0 = p\bar{e}\bar{e}_d + \left(\alpha_r L_m / \lambda_{ref}\right) \frac{K}{\epsilon} \left(k_o \bar{\sigma} + \bar{e}\right) \bar{e}_d - \alpha_r \bar{e}_q - p\bar{e}\lambda_{ref}$$

$$(4.44)$$

$$0 = \frac{\mu K}{\varepsilon} \left( k_0 \bar{\sigma} + \bar{\omega}_{ref} \right) \bar{e}_d + \mu \left( \frac{\lambda_{ref}}{L_m} - \frac{K \alpha_r/p}{\varepsilon} \right) \bar{e}_q - \left( b + \mu \frac{K}{\varepsilon} \lambda_{ref} \right) \bar{e}$$

$$-\left(\mu \frac{Kk_0}{\varepsilon} \lambda_{ref}\right) \bar{\sigma} - \left(b\bar{\omega}_{ref} + \bar{T}_L/m\right) \tag{4.45}$$

$$0 = \left(\frac{\lambda_{ref} - \bar{\epsilon}_d}{\lambda_{ref}}\right)\bar{e} - \frac{\bar{\omega}_{ref}}{\lambda_{ref}}\bar{e}_d + \frac{\alpha_r}{p\lambda_{ref}}\bar{e}_q \tag{4.46}$$

Naturally, the desired equilibrium point for the system is when the flux estimation errors  $\bar{e}_d = \bar{e}_q = 0$  and the speed error  $\bar{e} = 0$ , which imply that the output  $\omega$  tracks the reference input  $\omega_{ref}$ . Substituting these values in equation (4.45) provides the value

of  $\sigma$  at the desired equilibrium point as

$$\bar{\sigma} = \frac{-\varepsilon}{\mu K k_0 \lambda_{ref}} \left( b \bar{\omega}_{ref} + \bar{T}_L / m \right) \tag{4.47}$$

Linearizing equations (4.39)-(4.42) about the equilibrium point  $(e_d = e_q = e = 0, \sigma = \bar{\sigma})$ , we get the linear time-varying system

$$\dot{x} = \Lambda(t)x$$

where

$$\dot{x} = \begin{pmatrix} \dot{e_d} & \dot{e_q} & \dot{\sigma} & \dot{e} \end{pmatrix}^T$$
 $x = \begin{pmatrix} e_d & e_q & \sigma & e \end{pmatrix}^T$ 

and 
$$\Lambda(t) = \begin{pmatrix} -\alpha_r & -\frac{\alpha_r L_m K k_0}{\varepsilon \lambda_{ref}} \bar{\sigma} & 0 & 0 \\ \frac{\alpha_r L_m K k_0}{\varepsilon \lambda_{ref}} \bar{\sigma} & -\alpha_r & 0 & -p \lambda_{ref} \\ -\frac{\omega_{ref}}{\lambda_{ref}} & \frac{\alpha_r}{p \lambda_{ref}} & 0 & 1 \\ \frac{\mu K}{\varepsilon} \left( k_0 \bar{\sigma} + \omega_{ref} \right) & \mu \left( \frac{\lambda_{ref}}{L_m} - \frac{K \alpha_r / p}{\varepsilon} \right) & -\left( \mu \frac{K k_0}{\varepsilon} \lambda_{ref} \right) & -\left( b + \mu \frac{K}{\varepsilon} \lambda_{ref} \right) \end{pmatrix}$$

Substituting the value of  $\bar{\sigma}$  from equation (4.47) yields

$$\Lambda(t) = \begin{pmatrix} -\alpha_{r} & \frac{\alpha_{r}L_{m}}{\mu\lambda_{ref}^{2}} \left(b\bar{\omega}_{ref} + \frac{\bar{T}_{L}}{m}\right) & 0 & 0 \\ -\frac{\alpha_{r}L_{m}}{\mu\lambda_{ref}^{2}} \left(b\bar{\omega}_{ref} + \frac{\bar{T}_{L}}{m}\right) & -\alpha_{r} & 0 & -p\lambda_{ref} \\ -\frac{\omega_{ref}}{\lambda_{ref}} & \frac{\alpha_{r}}{p\lambda_{ref}} & 0 & 1 \\ \frac{\mu K\omega_{ref}}{\varepsilon} - \frac{1}{\lambda_{ref}} \left(b\bar{\omega}_{ref} + \frac{\bar{T}_{L}}{m}\right) & \mu\left(\frac{\lambda_{ref}}{L_{m}} - \frac{K\alpha_{r}/p}{\varepsilon}\right) & -\mu\frac{Kk_{0}}{\varepsilon}\lambda_{ref} & -b - \frac{\mu K\lambda_{ref}}{\varepsilon} \end{pmatrix}$$

Assuming that  $\omega_{ref}(t)$  and  $T_L(t)$  approach constant limits as  $t \to \infty$ , i.e.  $\lim_{t \to \infty} \omega_{ref}(t) = \bar{\omega}_{ref}$  and  $\lim_{t \to \infty} T_L(t) = \bar{T}_L$ ,  $\Lambda(t)$  constitutes a linear time-varying

system of the form

$$\Lambda(t) = A_1 + B_1(t)$$

where

$$A_{1} \ = \ \begin{pmatrix} -\alpha_{r} & \frac{\alpha_{r}L_{m}}{\mu\lambda_{ref}^{2}} \left(b\bar{\omega}_{ref} + \frac{\bar{T}_{L}}{m}\right) & 0 & 0 \\ -\frac{\alpha_{r}L_{m}}{\mu\lambda_{ref}^{2}} \left(b\bar{\omega}_{ref} + \frac{\bar{T}_{L}}{m}\right) & -\alpha_{r} & 0 & -p\lambda_{ref} \\ -\frac{\bar{\omega}_{ref}}{\lambda_{ref}} & \frac{\bar{\alpha}_{r}}{p\lambda_{ref}} & 0 & 1 \\ \frac{\mu K\bar{\omega}_{ref}}{\varepsilon} - \frac{1}{\lambda_{ref}} \left(b\bar{\omega}_{ref} + \frac{\bar{T}_{L}}{m}\right) & \mu \left(\frac{\lambda_{ref}}{L_{m}} - \frac{K\alpha_{r}/p}{\varepsilon}\right) & -\mu \frac{Kk_{0}}{\varepsilon}\lambda_{ref} & -b - \frac{\mu K\lambda_{ref}}{\varepsilon} \end{pmatrix}$$

$$B_{1}(t) = \begin{pmatrix} 0 & 0 & 0 & 0 \\ 0 & 0 & 0 & 0 \\ -\frac{\tilde{\omega}_{ref}}{\lambda_{ref}} & 0 & 0 & 0 \\ \frac{\mu K \tilde{\omega}_{ref}}{\varepsilon} & 0 & 0 & 0 \end{pmatrix}$$

where  $\bar{\omega}_{ref} = \omega_{ref} - \bar{\omega}_{ref}$ ,  $A_1$  is constant and  $B_1(t)$  is time-varying such that  $\lim_{t\to\infty} B_1(t) = 0$ . The above system can be viewed as a perturbed system where  $A_1$  is the system matrix of the nominal linear system and  $B_1(t)$  is the perturbation term. Theory of stability of perturbed systems [7, Example: 9.6] shows that if the origin is an exponentially stable equilibrium point of the nominal system

$$\dot{x} = A_1 x$$

and if

$$B_1(t) \to 0$$
 as  $t \to \infty$ 

then the origin is an exponentially stable equilibrium point of the perturbed system  $\dot{x} = \Lambda(t)x$ .

In order to investigate the stability of  $(e_d = e_q = e = 0, \sigma = \bar{\sigma})$  as an asymptotically stable equilibrium point for the system (4.39)-(4.42), we proceed with the calculation of the eigenvalues of the matrix  $A_1$ , which can be represented in the singularly perturbed form

$$P = \begin{pmatrix} P_{11} & P_{12} \\ \frac{P_{21} + \varepsilon \Delta_1}{\varepsilon} & \frac{P_{22} + \varepsilon \Delta_2}{\varepsilon} \end{pmatrix}$$

where

$$P_{11} = \begin{pmatrix} -\alpha_{r} & \frac{\alpha_{r}L_{m}}{\mu\lambda_{ref}^{2}} \left(b\bar{\omega}_{ref} + \frac{\bar{T}_{L}}{m}\right) & 0 \\ -\frac{\alpha_{r}L_{m}}{\mu\lambda_{ref}^{2}} \left(b\bar{\omega}_{ref} + \frac{\bar{T}_{L}}{m}\right) & -\alpha_{r} & 0 \\ -\frac{\bar{\omega}_{ref}}{\lambda_{ref}} & \frac{\alpha_{r}}{p\lambda_{ref}} & 0 \end{pmatrix}$$

$$P_{12} = \begin{pmatrix} 0 & -p\lambda_{ref} & 1 \end{pmatrix}^{T}$$

$$P_{21} = \begin{pmatrix} \mu K\bar{\omega}_{ref}, & -\mu K\alpha_{r}/p, & -\mu Kk_{0}\lambda_{ref} \end{pmatrix}$$

$$P_{22} = \begin{pmatrix} -\mu K\lambda_{ref} \end{pmatrix}$$

$$\varepsilon\Delta_{1} = \varepsilon \begin{pmatrix} -\frac{1}{\lambda_{ref}} \left(b\bar{\omega}_{ref} + \frac{\bar{T}_{L}}{m}\right), & \mu\lambda_{ref}/L_{m}, & 0 \right) \simeq O(\varepsilon)$$

$$\varepsilon\Delta_{2} = \varepsilon \begin{pmatrix} -b \end{pmatrix} \simeq O(\varepsilon)$$

The eigenvalues of this matrix can be approximated, for sufficiently small  $\varepsilon$ , by those of the matrices  $P_{11} - P_{12}P_{22}^{-1}P_{21}$  and  $P_{22}/\varepsilon$  [7].

It can be verified that

$$P_{12}P_{22}^{-1}P_{21} = \begin{pmatrix} 0 & 0 & 0 \\ -p\bar{\omega}_{ref} & -\alpha_r & -pk_0\lambda_{ref} \\ -\frac{\bar{\omega}_{ref}}{\lambda_{ref}} & \frac{\alpha_r}{p\lambda_{ref}} & k_0 \end{pmatrix}$$

and

$$P_{11} - P_{12}P_{22}^{-1}P_{21} = \begin{pmatrix} -\alpha_r & \frac{\alpha_r L_m}{\mu \lambda_{ref}^2} \left( b\bar{\omega}_{ref} + \frac{\bar{T}_L}{m} \right) & 0 \\ -\frac{\alpha_r L_m}{\mu \lambda_{ref}^2} \left( b\bar{\omega}_{ref} + \frac{\bar{T}_L}{m} \right) - p\bar{\omega}_{ref} & 0 & pk_0 \lambda_{ref} \\ 0 & 0 & -k_0 \end{pmatrix}$$

$$P_{22}/\varepsilon = -\mu \frac{K}{\varepsilon} \lambda_{ref}$$

and from these we see that there is a fast eigenvalue at  $-\mu \frac{K}{\varepsilon} \lambda_{ref}$  and a slow eigenvalue at  $-k_0$ . The remaining slow eigenvalues of  $A_1$  are the eigenvalues of the 2x2 matrix

$$A_{c} = \begin{pmatrix} -\alpha_{r} & \frac{\alpha_{r}L_{m}}{\mu\lambda_{ref}^{2}} \left(b\bar{\omega}_{ref} + \frac{\bar{T}_{L}}{m}\right) \\ -\frac{\alpha_{r}L_{m}}{\mu\lambda_{ref}^{2}} \left(b\bar{\omega}_{ref} + \frac{\bar{T}_{L}}{m}\right) - p\bar{\omega}_{ref} & 0 \end{pmatrix}$$

$$\lambda I - A_c = \begin{pmatrix} \lambda + \alpha_r & \frac{-\alpha_r L_m}{\mu \lambda_{ref}^2} (b \bar{\omega}_{ref} + \frac{\bar{T}_L}{m}) \\ p \bar{\omega}_{ref} + \frac{\alpha_r L_m}{\mu \lambda_{ref}^2} (b \bar{\omega}_{ref} + \frac{\bar{T}_L}{m})] & \lambda \end{pmatrix}$$

which gives

$$\left|\lambda I - A_c\right| = \lambda(\lambda + \alpha_r) + \left[p\bar{\omega}_{ref} + \frac{\alpha_r L_m}{\mu \lambda_{ref}^2} (b\bar{\omega}_{ref} + \frac{\bar{T}_L}{m})\right] \left[\frac{\alpha_r L_m}{\mu \lambda_{ref}^2} (b\bar{\omega}_{ref} + \frac{\bar{T}_L}{m})\right]$$

or

$$\left|\lambda I - A_c\right| = \lambda^2 + \alpha_r \lambda + \left[p\bar{\omega}_{ref}\kappa + \kappa^2\right]$$

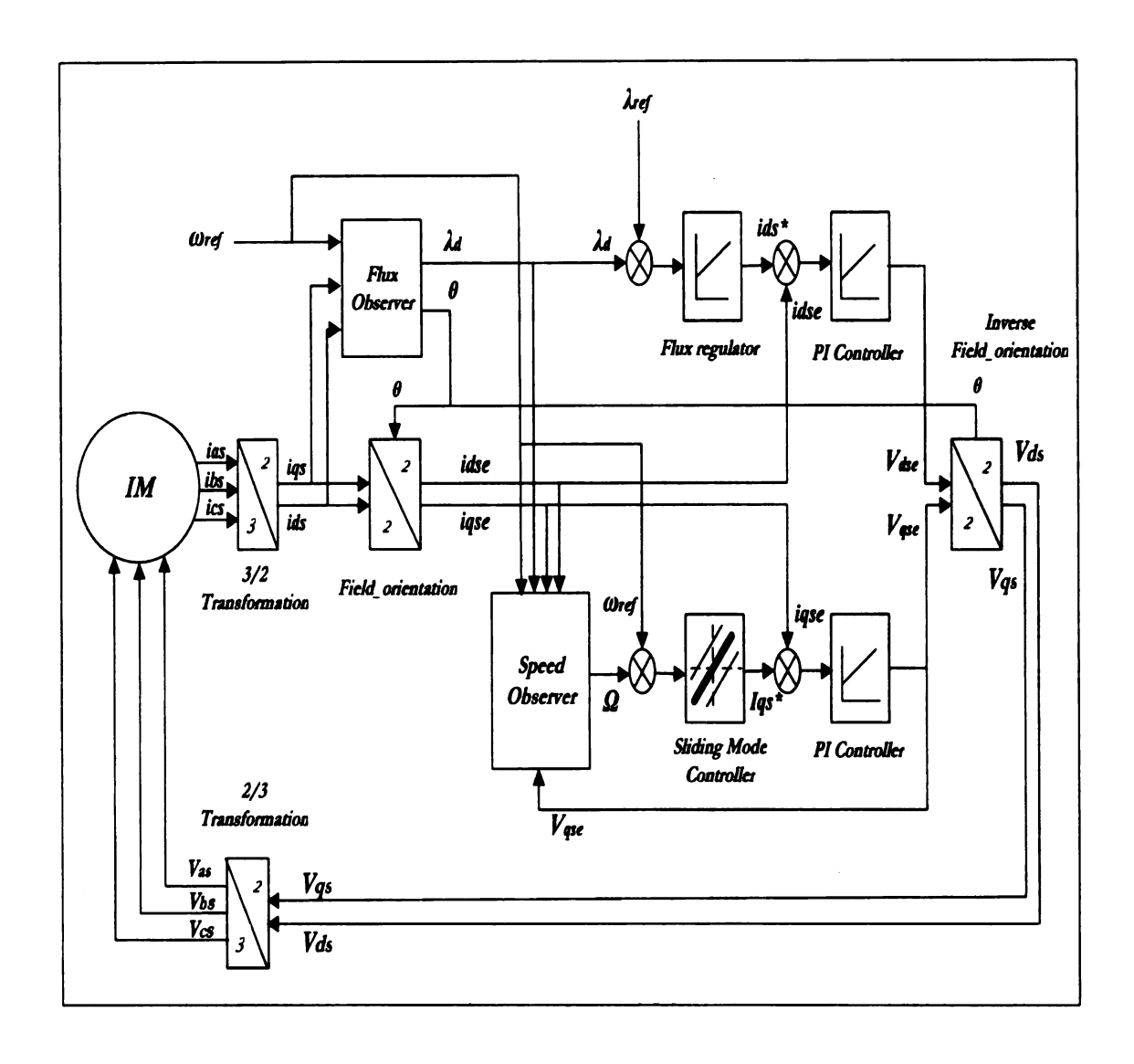


Figure 4.3. Sensorless control of an induction motor using sliding mode controller

where

$$\kappa = \frac{\alpha_r L_m}{\mu \lambda_{ref}^2} (b \bar{\omega}_{ref} + \frac{\bar{T}_L}{m})$$

The eigenvalues of  $A_c$ 

$$\lambda_{1,2} = -\frac{\alpha_r}{2} \pm \frac{1}{2} \sqrt{\alpha_r^2 - 4 \Big[ p \bar{\omega}_{ref} \kappa + \kappa^2 \Big]}$$

have negative real parts only when the product  $\kappa(p\bar{\omega}_{ref} + \kappa) > 0$ , which is the case when the steady-state speed command  $\bar{\omega}_{ref}$  and the steady-state load torque  $\bar{T}_L$  both have the same sign, positive or negative. The same condition was obtained in section 4.2.1, while investigating the stability of the zero dynamics of the system.

A Schematic for sensorless control of an induction motor using sliding mode control is presented in Figure 4.3.

# CHAPTER 5

## **Simulations**

The performance of the sliding mode controller is evaluated through simulations in the following sections. These simulations provide a way to compare the performance of the previously developed speed control algorithm using the traditional PI controllers with the sliding mode controller developed in Chapter 4.

# 5.1 Performance Comparison - PI controller vs Sliding Mode Controller

In order to examine the performance of the sliding mode controller, the simulations are performed considering the operation of induction motor under different conditions of parameter variations, load torque and reference speed variations. In this section, we present the comparison simulations where the performance of the sliding mode controller is compared with the traditional PI controller for the speed control of induction motor. For the purpose of this analysis, the induction motor is operated under similar conditions except that the speed controller is either a PI controller or a sliding mode controller. The simulation plots for the two controllers appear side by side representing the similar conditions being taken into consideration.

In order to obtain concrete conclusions about the performance of the two speed control algorithms, two induction motors, with different power ratings and machine parameters, have been simulated. However, the simulation results for only one of the induction motors are presented in this section. Simulation results for the other induction motor are available in the form of a compact disc.

### 5.1.1 Designing PI Controllers for the Speed Control

In this section, the PI controller gains are designed for two different induction motors, nicknamed as IM-1 and IM-2.

#### **Induction Motor IM-1**

The induction motor with the following machine parameters and ratings is used for the purpose of simulations:(Taken from [7, Example 5.6]):

200V, 4 pole, 3-phase, 60 Hz, Y-connected, Base Power 5 hp  $R_s = 0.183\Omega, R_r = 0.277\Omega, L_m = 0.0538H, L_s = 0.0553H, L_r = 0.056H, m = 0.0165Kg - m^2.$ 

A friction coefficient of  $b_1 = 0.01Kg - m^2/sec$  has been added.

#### Designing PI controller gains for IM-1

The gains of the PI controllers for IM-1 have been taken from [8]. These gains have been designed while considering the nominal parameters i.e.  $\hat{R}_r = R_r$  and  $\hat{R}_s = R_s$ .

The constants  $K_{dp}$  and  $K_{di}$  of the PI controller of  $v_d$  are chosen using the model

$$\frac{di_d}{dt} = -(\alpha_s \eta + \alpha_r \beta L_m)i_d + \gamma v_d + d_1 = -121.393i_d + 276.345v_d + d_1$$

where  $d_1$  is a disturbance input. The choice  $K_{dp}=20$  and  $\frac{K_{di}}{K_{dp}}=5$  assigns the closed-loop poles at  $-5.643 \times 10^3$  and  $-0.0049 \times 10^3$ . The magnitude of the transfer

function from the command input  $i_d^*$  to  $i_d$  is almost 0 dB over the frequency band  $[0,10^3]$  rad/sec, and the magnitude of transfer function from  $d_1$  to  $i_d$  is less than -30 dB over the frequency band  $[0,10^2]$  rad/sec.

The constants  $K_{fp}$  and  $K_{fi}$  of the PI controller of  $i_d$  are chosen using the model

$$\frac{d\lambda_d}{dt} = -\alpha_r \lambda_d + \alpha_r L_m i_d = -4.946\lambda_d + 0.266i_d$$

To ensure monotonic response of  $\lambda_d$ ,  $\frac{K_{fi}}{K_{fp}}=5$  has been taken to assign the zero of the PI controller at -5 (almost cancelation of the pole at -4.946). The gain  $K_{fp}$  has been chosen as  $K_{fp}=20$ , which assigns the closed-loop poles at  $-5.13\pm j0.48$ .

The constants  $K_{qp}$  and  $K_{qi}$  of the PI controller of  $v_q$  are chosen using the model

$$\frac{di_q}{dt} = -(\alpha_s \eta + \alpha_\tau \beta L_m + \alpha_r)i_q + \gamma v_q + d_2 = -121.393i_d + 276.345v_q + d_2$$

where  $d_2$  is a disturbance input. The choice  $K_{qp} = K_{qi} = 300$  assigns the closed-loop poles at  $-2.776 \times 10^4$  and -0.995. The magnitude of the transfer function from the command input  $i_q^*$  to  $i_q$  is almost 0 dB over the frequency band  $[0, 10^4]$  rad/sec, and the magnitude of transfer function from  $d_2$  to  $i_q$  is less than -30 dB over the frequency band [0, 900] rad/sec.

The constants  $K_{wp}$  and  $K_{wi}$  of the PI controller of  $i_q$  are chosen using the model (3.20)-(3.23). The transfer function of the linearization at the equilibrium point (3.28) is given by

$$G(s) = \frac{52.4(s^2 + 4.9464s + 0.887w_c\bar{i_q})}{(s + 0.6)[(s + 4.9464)^2 + (0.887\bar{i_q})^2] + 584.416(s + 4.9464 - o.159\bar{i_q}^2)}$$

The transfer function depends on the equilibrium point. By considering a range of possible values of  $\omega_{ref}$  and  $T_L$ , the controller gains were chosen as  $K_{wp} = K_{wi} = 30$ .

#### **Induction Motor IM-2**

The induction motor with the following machine parameters and ratings is used for the purpose of simulations:(Taken from [12]):

220V, 4 pole, 3-phase, 60 Hz, Y-connected, Base Power 3 hp Base Torque 11.9 N.m. , Base Current 5.8 Ampere, 1710rpm  $R_s = 0.435\Omega, R_r = 0.6531\Omega, L_m = 0.0693H, L_s = 0.0694H, L_r = 0.0696H,$   $m = 0.0189Kg - m^2.$ 

A friction coefficient of  $b_1 = 0.01 Kg - m^2/sec$  has been added.

#### Designing PI controller gains for IM-2

The gains of the PI controllers have been designed while considering the nominal parameters i.e.  $\hat{R_r} = R_r$  and  $\hat{R_s} = R_s$ .

The constants  $K_{dp}$  and  $K_{di}$  of the PI controller of  $v_d$  are chosen using the model

$$\frac{di_d}{dt} = -(\alpha_s \eta + \alpha_r \beta L_m)i_d + \gamma v_d + d_1 = -2715i_d + 2508.1v_d + d_1$$

where  $d_1$  is a disturbance input. The choice  $K_{di} = K_{dp} = 100$  assigns the closed-loop poles at  $-2.5 \times 10^5$  and  $-0.0099 \times 10^2$ . The magnitude of the transfer function from the command input  $i_d^*$  to  $i_d$  is almost 0 dB over the frequency band  $[0, 10^4]$  rad/sec, and the magnitude of transfer function from  $d_1$  to  $i_d$  is less than -30 dB over the frequency band  $[0, 10^3]$  rad/sec.

The constants  $K_{fp}$  and  $K_{fi}$  of the PI controller of  $i_d$  are chosen using the model

$$\frac{d\lambda_d}{dt} = -\alpha_r \lambda_d + \alpha_r L_m i_d = -9.3836\lambda_d + 0.6502i_d$$

and the choice  $K_{fp} = 50$  and  $K_{fi} = 100$  assigns he closed-loop poles at -203.48 and -0.981. The latter causes an almost cancelation of the zero at -1.00.

The constants  $K_{qp}$  and  $K_{qi}$  of the PI controller of  $v_q$  are chosen using the model

$$\frac{di_q}{dt} = -(\alpha_s \eta + \alpha_r \beta L_m + \alpha_r)i_q + \gamma v_q + d_2 = -2724.365i_d + 2508.1v_q + d_2$$

where  $d_2$  is a disturbance input. The choice  $K_{qp} = K_{qi} = 150$  assigns the closed-loop poles at  $-4.04 \times 10^5$  and -0.995. The magnitude of the transfer function from the command input  $i_q^*$  to  $i_q$  is almost 0 dB over the frequency band  $[0, 10^4]$  rad/sec, and the magnitude of transfer function from  $d_2$  to  $i_q$  is less than -30 dB over the frequency band  $[0, 10^2]$  rad/sec.

The constants  $K_{wp}$  and  $K_{wi}$  of the PI controller of  $i_q$  are chosen using the model (3.20)-(3.23). The transfer function of the linearization at the equilibrium point is given by

$$G(s) = \frac{20.1375(s^2 + 9.3836s + 2.16w_c i_q)}{(s + 0.1124)[(s + 9.3836)^2 + (2.1676i_q)^2] + 174.35(s + 9.3836 - 0.5i_q^2)}$$

The transfer function depends on the equilibrium point. By considering a range of possible values of  $\omega_{ref}$  and  $T_L$ , the controller gains were chosen as  $K_{wp} = K_{wi} = 300$ .

### 5.1.2 Sliding Mode Controller - Parameters

The PI controller gains have been designed for the two different motors; however, the same sliding mode controller is used in both cases.

The Sliding mode controller parameter K is defined based on the q-axis current requirement for the specific induction motor drive (which is proportional to the load torque  $T_L$ ). The typical value of  $i_q$  for a load torque command of 20 N.m. is approximately 25 Amperes, which suggests that the sliding mode controller parameter K should be taken around 30-35 for a very smooth operation under even

unpredictable load conditions. The value of constant gain  $k_0$  is chosen as unity. The signum function of the sliding mode controller is replaced with  $sat(\frac{s}{\varepsilon})$  and the value of  $\varepsilon$  is taken as 0.01.

### 5.1.3 Performance Comparison

In this section, we present the simulation plots for various cases in which the two controllers are studied for similar situations. The simulation plots appear side by side for the two controllers for the same situation and for the same induction motor.

The flux observer (3.4) is initiated at

$$\hat{\lambda}(0) = \left(\begin{array}{c} 0.1 \\ 0 \end{array}\right)$$

so that  $\lambda_d(0) = 0.1$ . The speed observer (3.16)-(3.17) is implemented with  $\alpha_1 = 2$ ,  $\alpha_2 = 1$ ,  $\varepsilon = 0.0002$ ,  $\hat{\mu} = \mu$  and  $\hat{b} = b$ . In the simulations, the components of  $v_s$  are limited to  $\pm V_{max}$  V. The speed reference varies for different situations, however, for a number of simulation cases, it is taken as a step input smoothed by the transfer function 1/(0.5s+1).

Figure 5.1 shows simulation results for the two controllers for a speed command of 100 rad/sec applied at zero time with a load of 20 N.m. applied between t=4 and t=8 sec. This simulation is for the nominal parameters case i.e.  $\hat{R_r}=R_r$  and  $\hat{R_s}=R_s$ . Clearly, both the controllers have equivalent performance curves for the nominal parameters case.

Figure 5.2 shows simulation results for the two controllers for a speed command of 100 rad/sec for the case when there is a 100 percent increase in the rotor resistance  $R_r$  and the nominal stator resistance i.e.  $\hat{R_s} = R_s$ . A load of 20 N.m. is

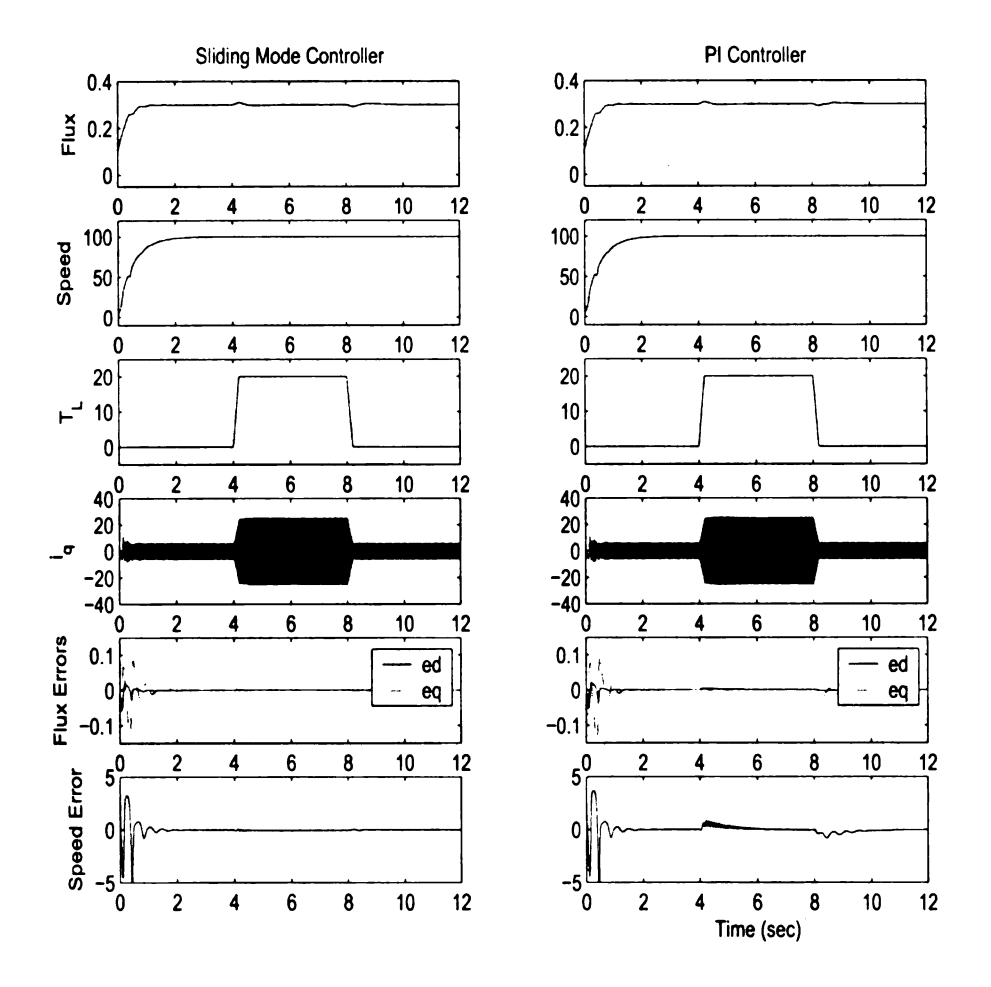


Figure 5.1. Simulation results with nominal parameters

applied between t = 4 and t = 8 sec.

According to (3.28), the equilibrium values are  $e_d=e_d=0$ , and

$$\bar{\omega} - \omega_{ref} = \frac{(\hat{\alpha}_r - \alpha_r) L_m \bar{i}_q}{p \lambda_{ref}} = -0.4435 \bar{i}_q$$

where

$$\bar{i}_q = \frac{b\omega_{ref} + T_L/m}{\mu\lambda_{ref} - \frac{b(\alpha r - \alpha_r)L_m}{p\lambda_{ref}}} = \frac{60.6061(1 + T_L)}{52.6714}$$

For  $T_L=20$ , we obtain  $\bar{i}_q=24.164$ . The simulation results confirm these calculations. The two controllers present almost equivalent performance for such parameter variation.

Figure 5.3 repeats the simulation for the two controllers for the speed com-

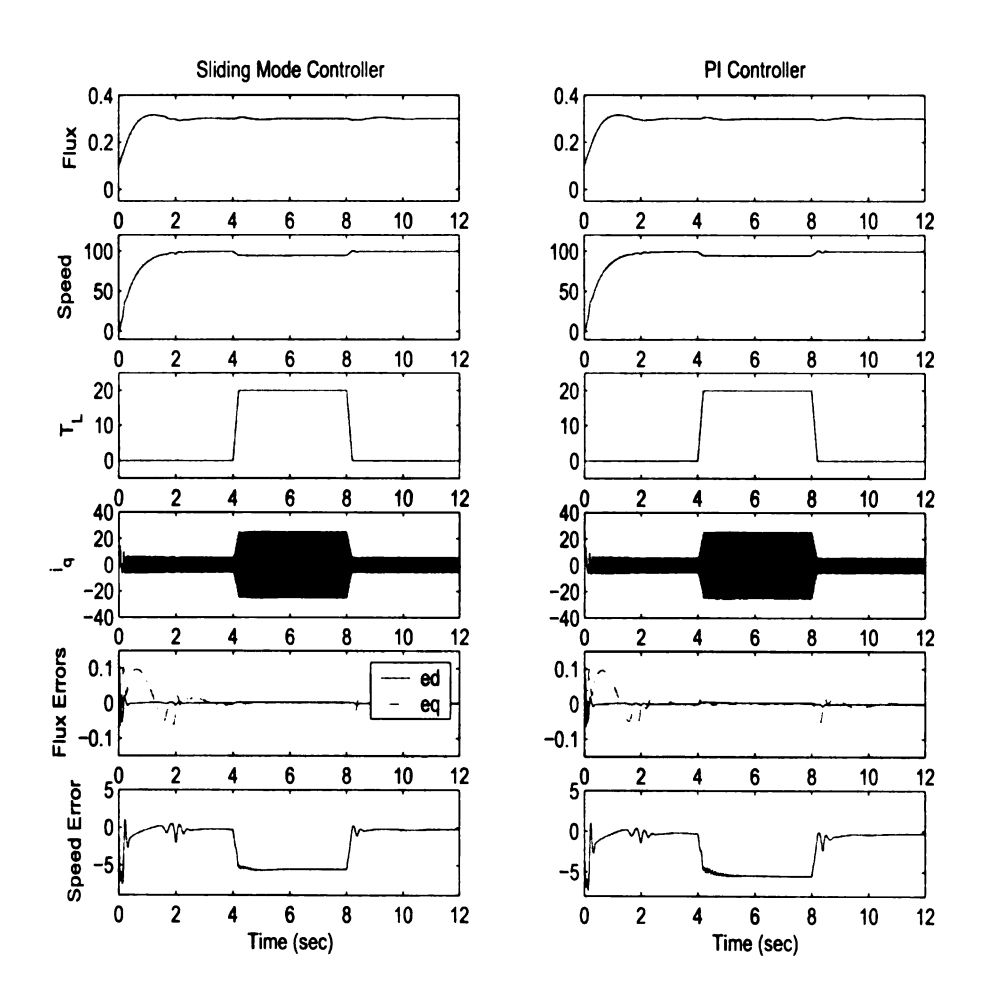


Figure 5.2. Simulation results with 100 percent increase in  $R_r$  and nominal  $R_s$ 

mand of 100 rad/sec, with a 100 percent increase in both the rotor resistance  $R_r$  and

the stator resistance  $R_s$ . In this case, we expect the equilibrium point to be slightly perturbed from the one we obtained in Figure 5.1.3. This is indeed the case. Clearly, in this case  $e_d$  and  $e_q$  are no longer zero. The sliding mode controller has a slight performance edge in this parameter variation case as it produces less speed error when the induction motor is subjected to the load.

Figure 5.4 shows speed reversal from 50 to -50 rad/sec at no load, with nomi-

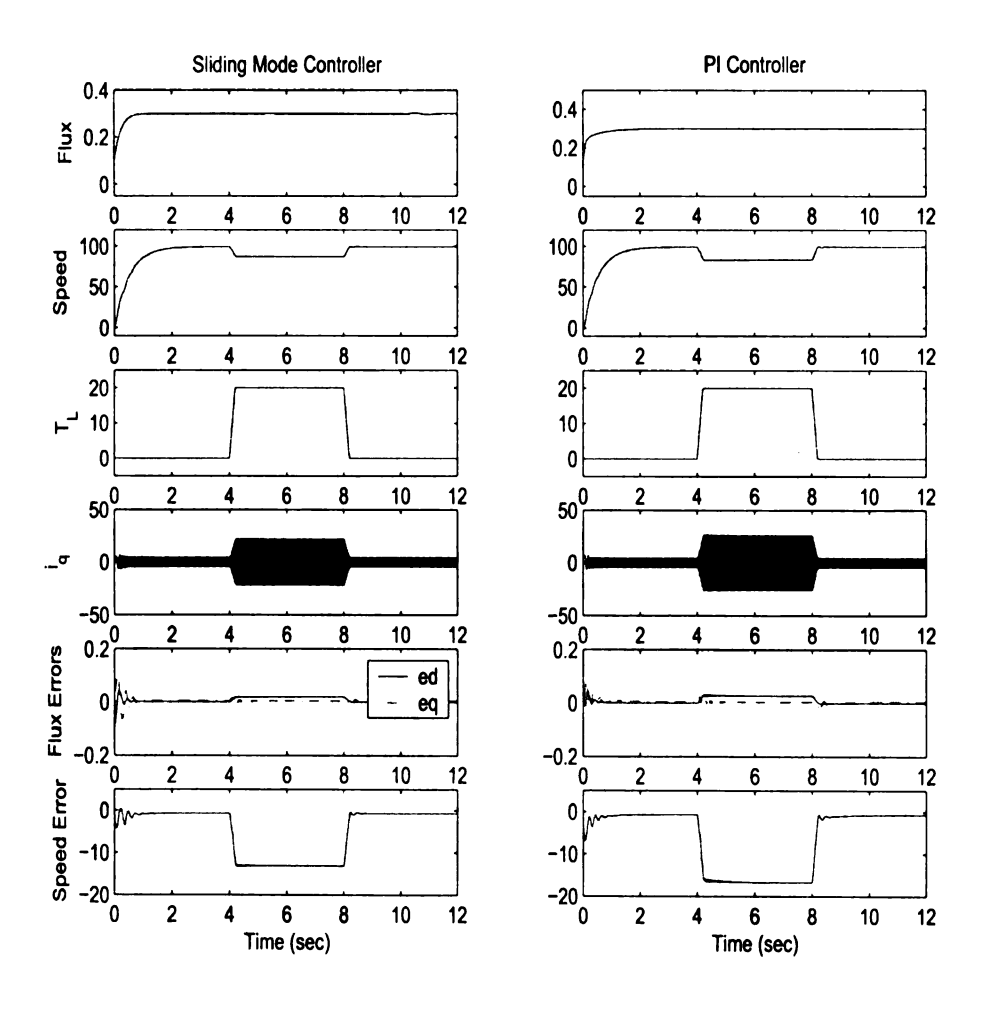


Figure 5.3. Simulation results with 100 percent increase in  $R_r$  and  $R_s$ 

nal parameters. It can be seen that the system settles back at the equilibrium point following a transient during speed reversal. The two controllers have almost the same performance for speed reversal from 50 to -50 rad/sec. The sliding mode controller has a slight edge as it produces less flux estimation error during the transient. The important factor that limits the performance is the control saturation. For both controllers, reversing the speed from 100 to -100 rad/sec causes a control saturation. During the control saturation the variables oscillate and the performance degrades significantly.

Figure 5.5 shows the simulation results for the case when the induction motor is subjected to a step load torque  $T_L$ =20 N.m. at time t = 4 seconds. This can be viewed as a case when a sudden load torque command is applied while the induction motor is operating under no load conditions before. Such cases can arise in practice under different drive fault conditions. It is clear from the simulation plots that the sliding mode controller has an edge over the PI controller in such situation.

Figure 5.6 supplements the results of Figure 5.5. This figure shows the simulation results for the case when the induction motor is subjected to a sudden step load torque  $T_L$  of a higher value for a short period of time after the induction motor has been subjected to  $T_L=20$  N.m. at t=4 seconds.

This case represents a fault condition in that the drive load rises higher than the nominal value for which the drive is designed. Such cases can arise in practice when two or more induction motors operate in parallel in a drive system and one or more of them suddenly go out of operation, resulting in a sudden load rise on the remaining machines within the drive system. It is clear from the simulation plots that the sliding mode controller outperforms the PI controller in such situation.

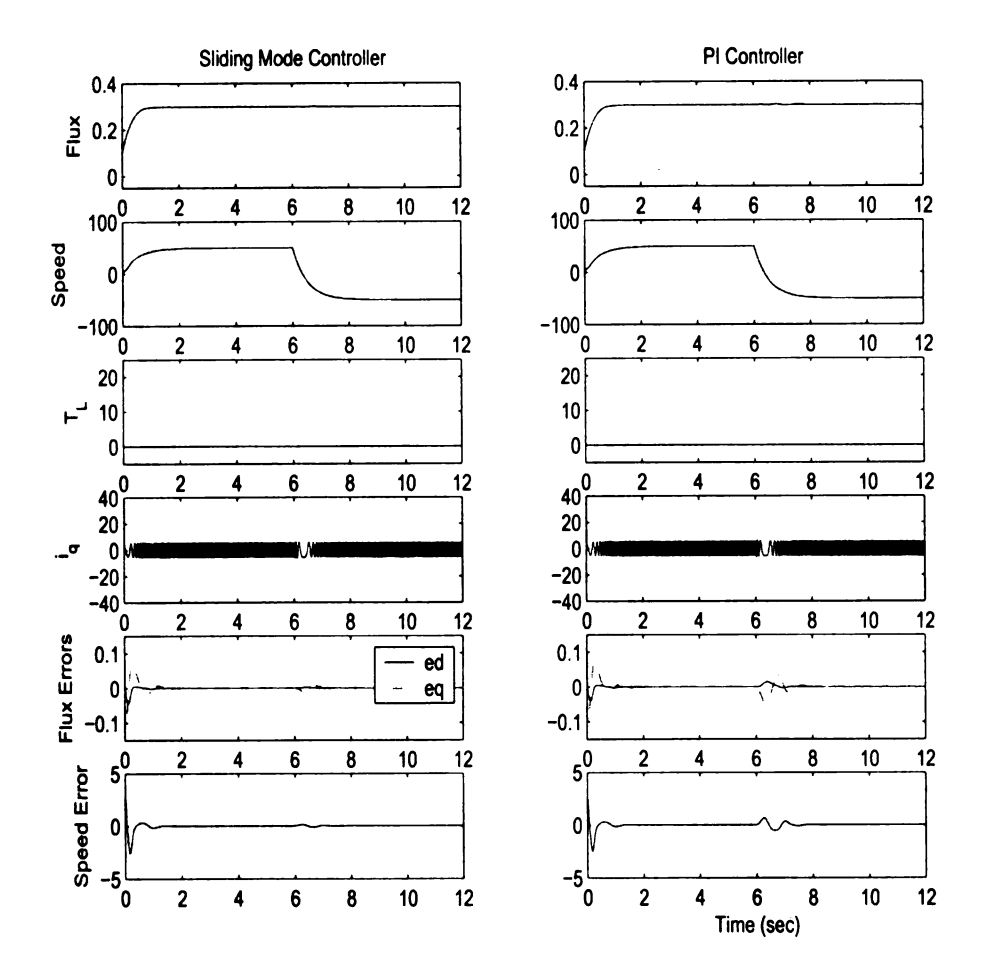


Figure 5.4. Simulation results for speed reversal under no load conditions with nominal parameters

Figure 5.7 demonstrates the importance of the condition  $\omega_c \bar{i}_q$  obtained in Chapter 3 and the similar condition  $\kappa(p\bar{\omega}_{ref} + \kappa) > 0$  obtained in Chapter 4. This condition is satisfied for all the cases discussed so far. In this case, we apply a speed command of 10 rad/sec at zero time. Then, at time t = 4, we apply a load of -1 N.m. For these values,  $\bar{i}_q = -1.1564$  and  $\omega_c = 18.9758$ ; hence,  $\omega_c \bar{i}_q < 0$ . Similarly, the term  $\kappa(p\bar{\omega}_{ref} + \kappa) > 0$  is violated in that for these values it turns out that  $\kappa(p\bar{\omega}_{ref} + \kappa) = -18.958 \neq 0$ . It is

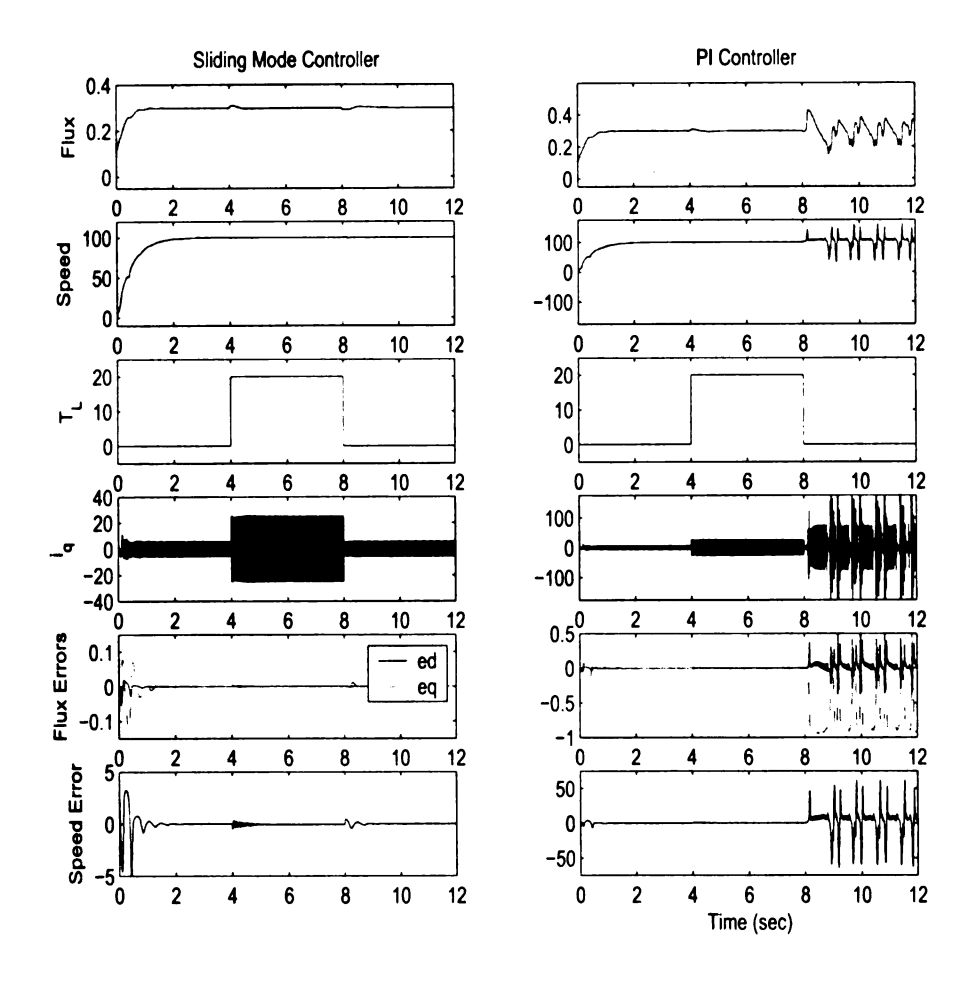


Figure 5.5. Simulation results for step load torque  $T_L$  with nominal parameters

clear from the simulation that the equilibrium has been destabilized after applying the load. However, notice that the sliding mode controller recovers the performance during the transient and eventually attains zero steady-state error. This simulation shows the edge the sliding mode controller has over the PI controller for its good performance against un-modeled dynamics, external disturbance rejection and fast dynamic response.

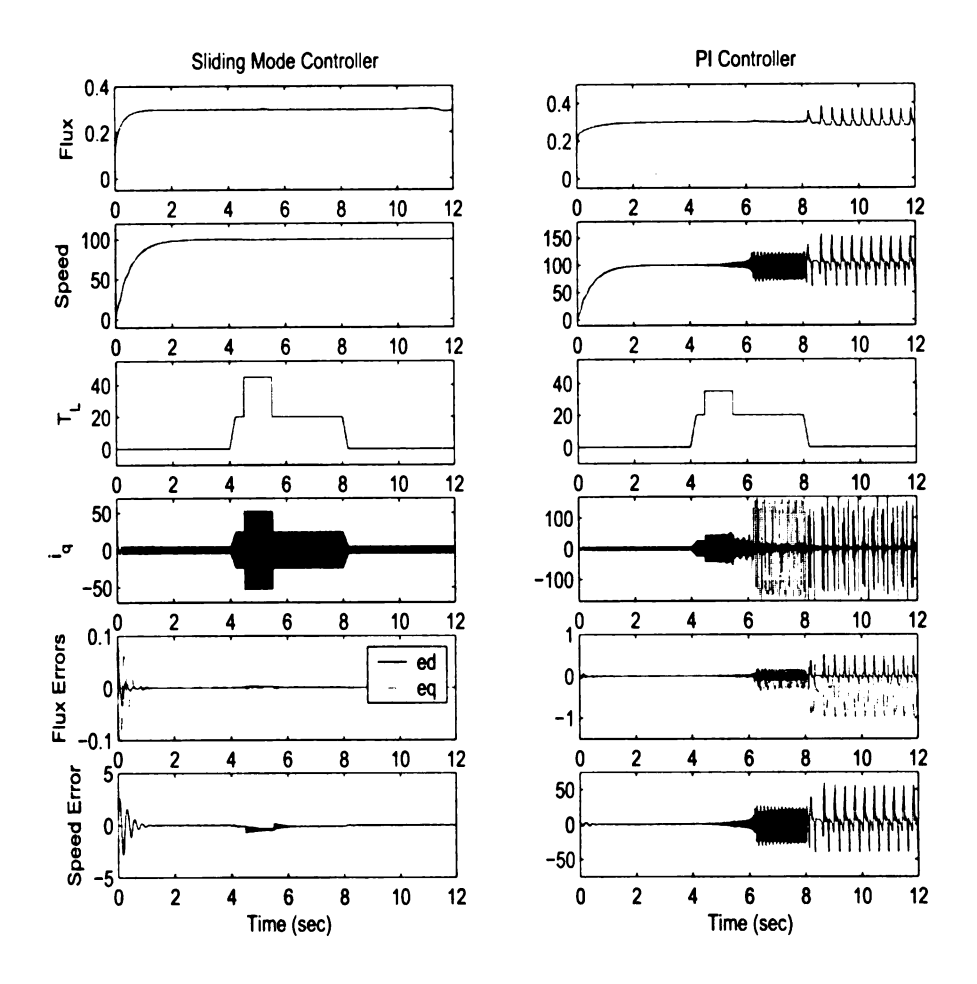


Figure 5.6. Simulation results for sudden step load torque increase with nominal parameters

Figure 5.8 shows the simulation results for the case when the induction motor is subjected to a step reference speed command of 75 rad/sec at time t=1 seconds. The sliding mode controller obediently tracks the reference speed after a short transient period in which the trajectories outside the boundary layer reach boundary layer and move inside it toward the equilibrium point, giving a zero steady-state error. The PI controller struggles through and the performance deteriorates with the passing seconds.

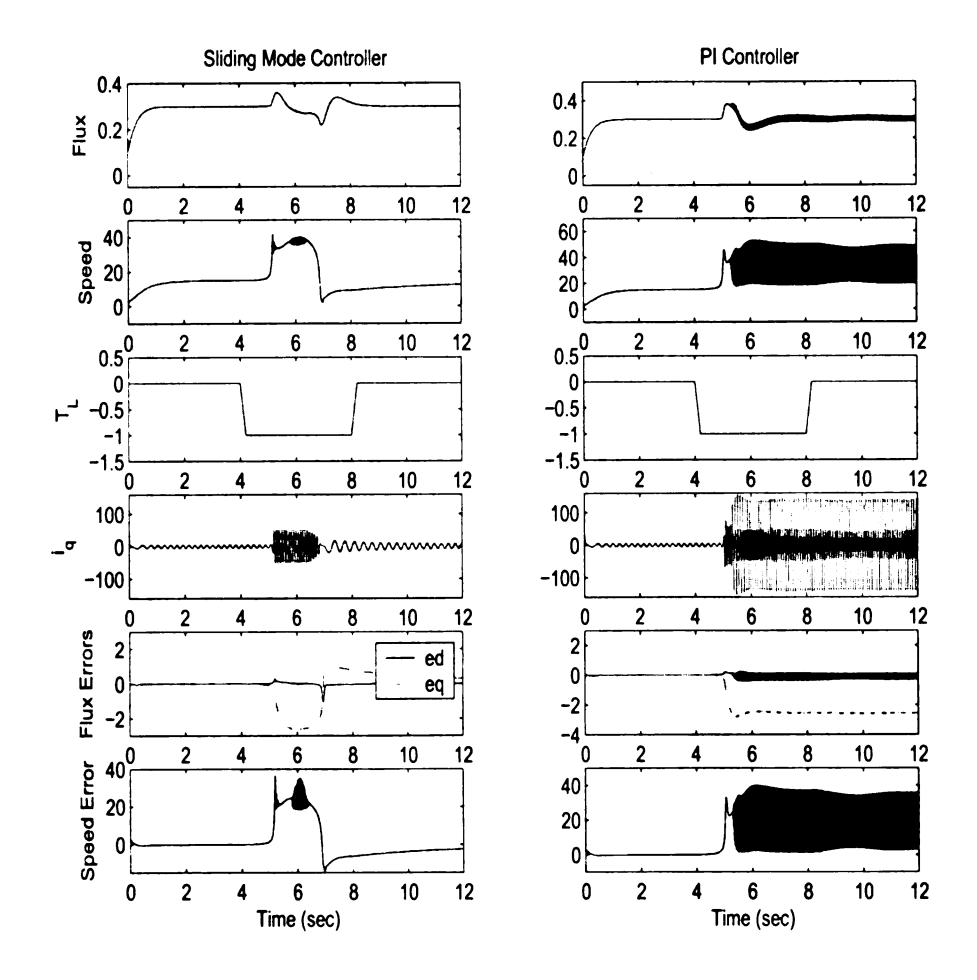


Figure 5.7. Simulation results demonstrating loss of stability in case of PI controller when under negative load torque with nominal parameters

Figure 5.9 presents the case when the induction motor has already attained a reference speed of 100 rad/sec. This represents the initial state of the system. Then, a negative speed step command of -15 rad/sec is applied. During the transient, the sliding mode controller recovers the performance while the PI controller loses stability and shows an increasing deterioration in performance. Notice that, the sliding mode controller also shows the speed error during the transient when the

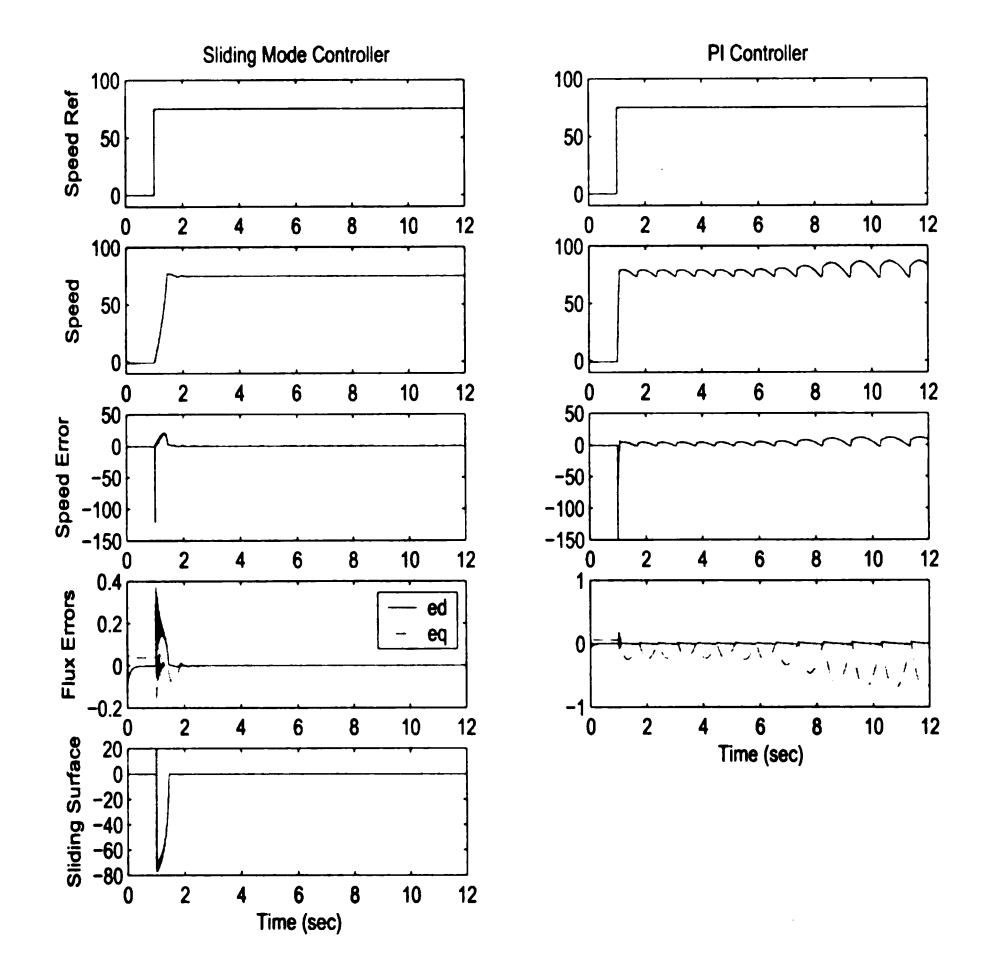


Figure 5.8. Simulation results for step speed command with nominal parameters

negative speed step is applied. This is due to the presence of the PI controller in the closed-loop that outputs the stator voltage as feed back to the induction motor. This PI controller

$$V_q = \frac{(K_{qp}s + K_{qi})}{s} [I_q^* - I_q]$$

regulates  $i_q$  to  $i_q^*$  and outputs the q-axis stator voltage as feedback in the closed-loop. Therefore, an error presented by this PI controller has a direct effect on the performance of the sliding mode controller.

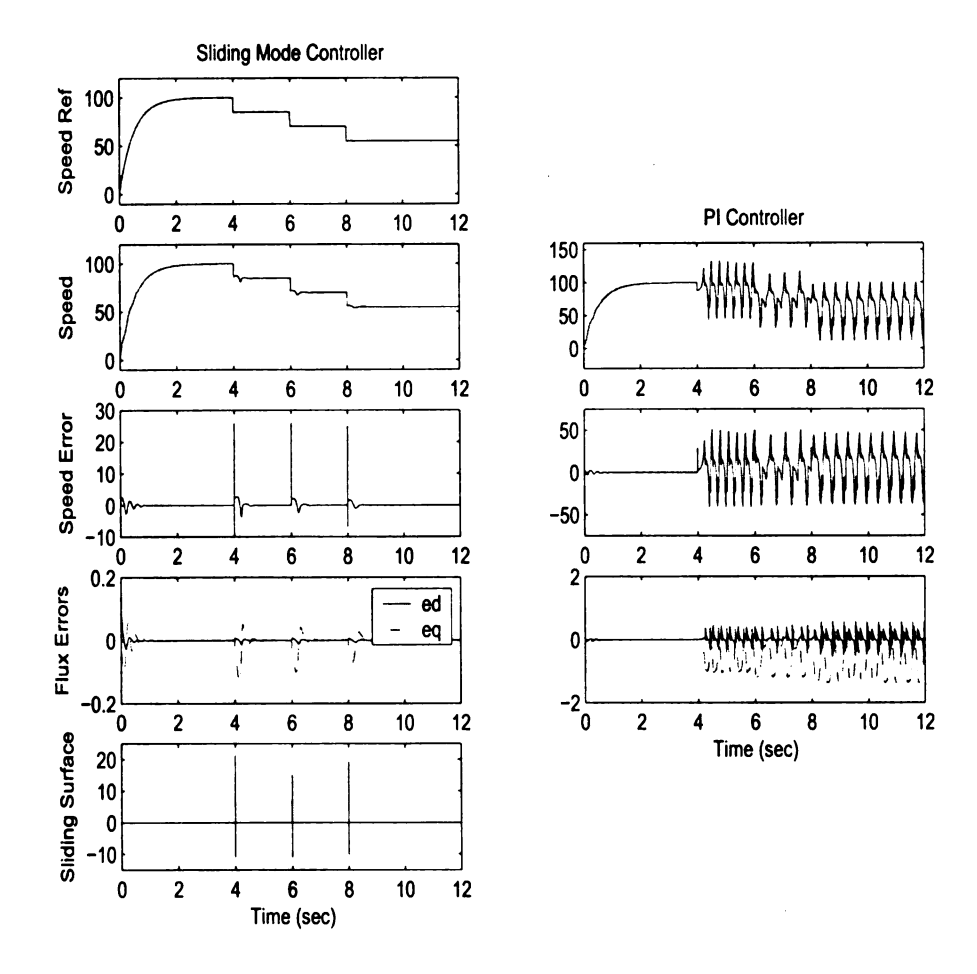


Figure 5.9. Simulation results for multi-step speed reduction with nominal parameters

Figure 5.10 supplements the results of the Figure. 5.9. This simulation also presents the case when the induction motor has already attained a reference speed of 100 rad/sec. Therefore the system is considered to have initial condition of operating at 100 rad/sec. Then, a monotonically decreasing speed reference is applied in such a way that the system attains the desired speed, say, 60 rad/sec at some pre-defined time. The simulation results show that the sliding mode controller

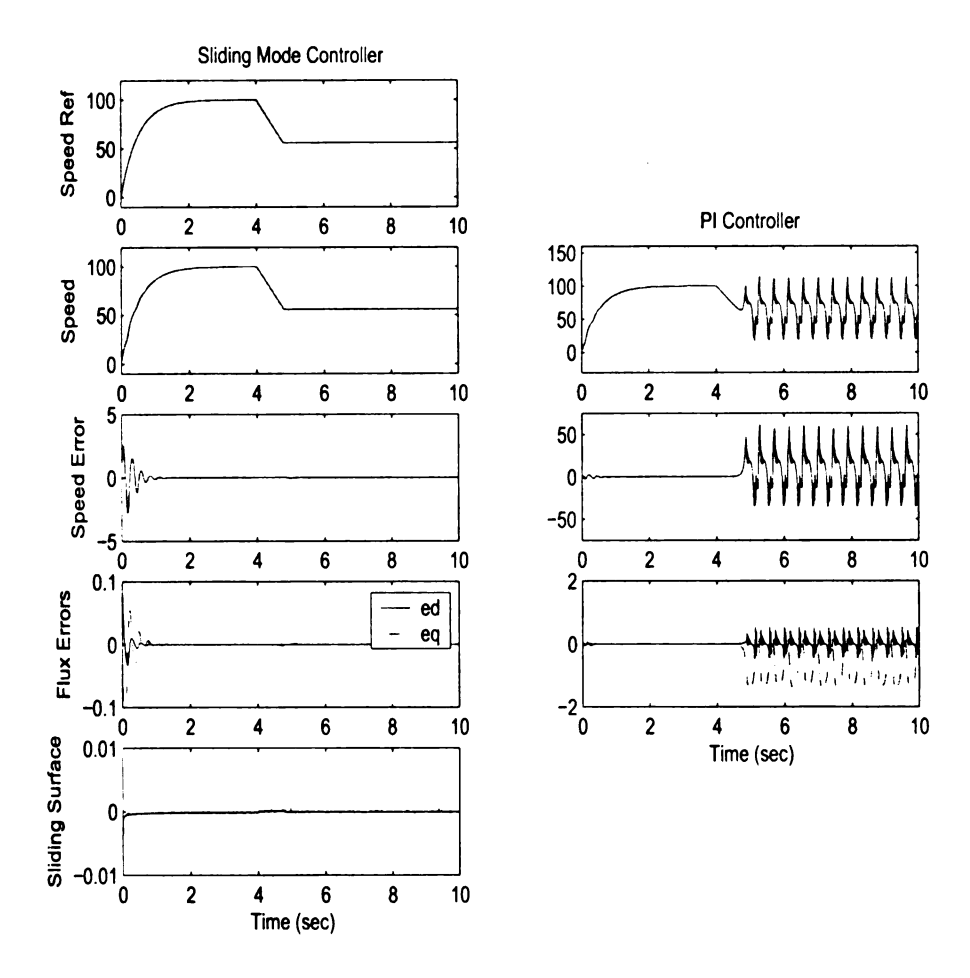


Figure 5.10. Simulation results for monotonic speed reduction command with nominal parameters

smoothly tracks the reference speed in this case while the performance of the PI controller deteriorates.

# CHAPTER 6

## **Conclusions**

Sensorless speed control of induction motors using flux and speed observers is an emerging technology, which is pushed forward by the need to develop low-cost, dependable drive systems. The induction motor presents a complex control problem due to its nonlinear dynamics and dependence upon parametric variations. In order to develop efficient sensorless induction motor drive systems, it is necessary to take into account the nonlinearities of the system.

A speed control algorithm based on sliding mode control strategy is presented in this work. This nonlinear controller replaces the traditional PI controller used for similar purposes. Analysis reveals the conditions under which the developed sliding mode controller provides effective speed control, while preserving the closed-loop system stability under uncertain external load disturbances and reference speed variations. A performance comparison presents the edge that the developed sliding mode controller has over the traditional PI controller.

Some aspects of the analysis of the sliding mode control has been restricted to local regions. A more elaborate nonlocal analysis would certainly provide better insight into the control problem, however, pursuing the same is not very clear.

In particular, performing nonlinear analysis requires the existence of a Lyapunov function, which is not transparent at this point.

Human nature has a tremendous drive to seek for the best. This work is a small step ahead of an earlier work [8], and there is a long way to go. The theoretical analysis has been supplemented by simulation results and the next step would be obtaining the experimental results.

# **BIBLIOGRAPHY**

### **BIBLIOGRAPHY**

- [1] A. N. Atassi and H. K.Khalil. A separation principle for the stablization of a class of nonlinear systems. *IEEE Trans. Automat. Contr.*, (44):1672-1687, 1999.
- [2] B. Aloliwi L. Laubinger E. G. Strangas, H. K. Khalil and J. Miller. Robust tracking controllers for induction motors without rotor position sensor: Analysis and experimental results. *IEEE Trans. Energy Conversion*, (14):1448–1458, 1999.
- [3] E.J.Davison. The robust control of a servomechanism problem for linear time-invariant multivariable systems. *IEEE Trans. Automat. Contr.*, 1(AC-21):25–34, 1976.
- [4] J. Holtz. Sensorless position control of induction motors-an emerging technology. *IEEE Trans. Ind. Electron.*, (45):840–852, 1998.
- [5] A. Isidori. Nonlinear Control Systems. Springer, 3rd edition, 1995.
- [6] A. Kawamura K. Rajashekara and K. Matsuse, editors. Sensorless Control of AC Motor Drives: Speed and Position Sensorless Operation. IEEE, 1996.
- [7] H. K. Khalil. *Nonlinear Systems*. Prentice Hall, Upper Saddle River, New Jersey, 3rd edition, 2002.
- [8] H. K. Khalil and E. G. Strangas. Sensorless speed control of induction motors. In Proc. American Control Conference, 2004.
- [9] R. Krishnan. *Electric Motor Drives*. Prentice Hall, Upper Saddle River, New Jersey, 2001.
- [10] W. Leonhard. Control of Electrical Drives. Springer, 2nd edition, 1996.
- [11] R. D. Lorenz. Advances in electric drive control. *International Conference on Electric Machines and Drives*, pages 9-16, 1996.
- [12] O. Wasynczuk P. C. Krause and S. D. Sudhoff. Analysis of Electrical Machinery and Drive Systems. John Wiley and Sons, New York, 2nd edition, 2002.

- [13] H. K. Khalil P. V. Kokotović and J. O'Reilly. Singular Perturbation Methods in Control: Analysis and Design. Academic Press, New York, 1986. Republished by SIAM, 1999.
- [14] P. Vas. Sensorless Vector and Direct Torque Control. Oxford University Press, London, 1998.
- [15] G. C. Verghese and S. R. Sanders. Observers for flux estimation in induction machines. *IEEE Trans. Ind. Electron.*, 1(35):85-94, 1988.

